SITE AMPLIFICATION ESTIMATION OF GARHWAL HIMALAYA USING HVSR AND S-WAVE METHOD

A DISSERTATION

Submitted in the partial fulfilment of the requirements for the award of the degree of

MASTER OF TECHNOLOGY

in

EARTHQUAKE ENGINEERING

(With Specialization in Structural Dynamics)

by

HIMANSHU SINGH

(17526008)

DEPARTMENT OF EARTHQUAKE ENGINEERING

INDIAN INSTITUTE OF TECHNOLOGY ROORKEE

ROORKEE – 247667, UTTARAKHAND, INDIA

June, 2019

CANDIDATE'S DECLARATION

I hereby, declare that the work which is being presented in this dissertation entitled, **"SITE AMPLIFICATION ESTIMATION OF GARHWAL HIMALAYA USING HVSR AND S-WAVE METHOD"**, being submitted in partial fulfilment of the requirements for the award of degree of "Master of Technology" in "Earthquake Engineering" with specialization in Structural Dynamics, to the Department of Earthquake Engineering, Indian Institute of Technology Roorkee, under the supervision of **Dr. S. C. Gupta**, Associate Professor, Department of Earthquake Engineering, Indian Institute of Technology Roorkee, is an authentic record of my own work carried out during the period of June 2018 to June 2019.

I declare that I have not submitted the material embodied in this dissertation for the award of any other degree or diploma.

Place: Roorkee **Himanshu Singh**

Date: Enrollment no. 17526008

CERTIFICATE

This is to certify that the above statement made by the candidate is correct to the best of my knowledge and belief.

Place: Roorkee **(Dr. S. C. Gupta)**

Date: Associate Professor

Department of Earthquake Engineering

Indian Institute of Technology Roorkee

ACKNOWLEDGEMENT

I wish to express my deep sense of gratitude and indebtedness to my guide and mentor **Dr. S.C. Gupta**, Associate Professor, IIT Roorkee for being helpful and great source of inspiration. I am thankful to him for his persistent interest, constant encouragement, vigilant supervision and critical evaluation. His helping nature, valuable suggestions and scholastic guidance are culminated in the form of the present work.

I would like to record my deep sense of gratitude to my encouraging parents and my family, without whose blessings and love the thesis would not have seen the daylight. I would also like to thank all my dear friends and classmates for their support.

Place: Roorkee **Himanshu Singh**

Date: Enrollment no. 17526008

ABSTRACT

Using high quality three-component digital data recorded on 12-stations, site amplifications have been estimated from spectral ratios of horizontal to vertical (H/V) recordings and S wave spectral ratio method. This study analyses data of 7 earthquakes ranging from M 3.0 to M 5.1, and depths from 4 to 38 km. Digital data recorded by 12 stations of seismological network around Tehri region operated by Department of Earthquake Engineering, IIT Roorkee and sponsored by THDC India Ltd. have been utilized. The noise part of the seismograms has been used for estimating site response and to extract the predominant peaks by the H/V method and the S-wave portion of seismogram is used for S-wave spectral ratio method. The amplifications determined from the H/V method are, however, different from the amplifications determined from the direct spectral ratio method.

H/V spectral ratios are computed from 201 waveforms in the frequency range 1 Hz to 12 Hz and S-wave spectral ratios are computed from 114 waveforms in the frequency range 1 Hz to 12 Hz considering PRAT located on the Quartzite rock as a reference.

Estimates of H/V spectral ratios has given dominant peaks between 2 Hz and 5 Hz at all sites, and beyond 5 Hz, no sharp amplification is observed. From S-wave spectral ratios, almost similar frequency dependent trends in the radial and transverse components has been revealed at the majority of the sites relative to PRAT site as a reference site and the dominant peaks are observed between 2 Hz and 6 Hz

High amplification at higher frequencies at CHAN and GIYA sites seems to be due to topographical effect, as the sites are located at the mountain peak. By and large at all the sites, the vertical components show consistently low site amplifications as compared to horizontal component.

TABLE OF CONTENTS

LIST OF FIGURES

LIST OF TABLES

Chapter-1 Introduction

1.1 General

Earthquakes occur without warning and can strike at any time. Violent ground shaking due to earthquake causes damage to structures and resulting loss of life. The earthquake intensity depends on many factors but at times even for small earthquakes, there is a varying degree of damage to the structures that may even lead to collapse of the structure. This is caused due to amplification of the ground motion. The properties and the geometrical configuration of soil layer influence the amplification of ground motion. A significant part of damage observed in destructive earthquakes around the world is associated with seismic wave amplification due to local site effects. Amplitudes of seismic waves increase significantly as they pass through soft soil layers near the earth's surface. The damage to the structures during some of the important earthquakes such as the great Mexico earthquake of 1985 and the Bhuj earthquake of 2001(Chopra et al., 2013) were investigated to be confined in the areas underlain by soft soil deposits. Many of these areas are along the margins of the Bay mud and are located as much as 350 km far from the epicenter of the earthquake. The increased amounts of damages were observed due to amplification effects of soft soil deposits on certain frequencies of ground shaking.

The earthquake source describes how the size and nature of earthquakes source mechanism controls the generation of seismic waves. The path effect describes the change in the amplitude and frequency contents of seismic waves by the earth's medium when the seismic waves travel from earthquake source to the recording station. The site effect describes the modification of ground motion due to the composition and configuration of local geological structure below the recording station (Boore and William, 1997).

The study of the effects of local site conditions is one of the most important goals of earthquake engineering. General seismic hazard evaluations are calculated over broad geographical areas; however, as more ground-motion data are collected, the local geologic site condition is emerging as one of the dominant factors controlling the variation in ground motion and determination of the site-specific seismic hazard. Damage to property and loss of life in earthquakes are frequently a direct result of the local site geological conditions affecting the incident ground motion. At present, however, the method by which site amplification is determined is still under investigation among seismologists and earthquake engineers.

It has long been known that each soil type responds differently when it is subjected to ground motion from earthquakes. These observations are made by comparing earthquake records taken from sites with different underlying soil types.

The most frequent empirical technique used for site-response estimation has been the S-wave spectral ratio method (Bonilla et al., 1997). This approach considers the ratio between the spectrum at a site of interest and the spectrum at a reference site, which is usually a nearby rock site.

Horizontal-to-vertical spectral ratio method was used to estimate site response to extract the predominant frequency (Arai and Tokimatsu, 2005).

1.2 Objectives

Objective of this study is to determine the site amplification characteristics due to weak ground motion recorded at stations of Garhwal Himalaya seismic network in the frequency range 1 Hz -12 Hz using H/V spectral ratio method and S-Wave spectral ratio method for frequency range 1 Hz -12 Hz

The study has been carried out for the following purpose:

1. For the frequency range of 1 Hz – 12 Hz, site amplification characteristics at 12 sites located in Garhwal Himalaya from the digitally recorded data.
2. To study the estimated site amplification with the site geology.

1.3 Region studied

For estimation of Site amplification of the region around Garhwal Himalaya is selected. Mild earthquakes occur in the region every year due to its location. The region is surrounded by major boundary thrusts, the Himalayan Frontal Thrust, the Main boundary Thrust, the Main Central Thrust lie in this region. The seismological record measurements suggest a significant seismic potential for the Garhwal Himalayan region. The region has experienced several recent moderate earthquakes and it continues to accumulate the strain and yet to release it in the form of great earthquake. The analysis of local events recorded by twelve station network shows that most of the seismic events recorded in this region continue to occur from shallow depths.

1.4 Organisation of Thesis

The thesis has been described into five chapters.

The layout plan for each chapter is as follows:

Chapter 1 includes the broad importance and objective of site amplification.

Chapter 2 incorporates a brief review of various methodologies used to estimate the site amplification. This chapter also gives a brief account of observations and interpretation of local site amplification characteristics with respect to the geology and topography in different seismic regions of the world.

Chapter 3 contains the seismological network and the data set used for estimating the site amplification using the H/V spectral ratio and S-wave ratio method on the digital recorded seismograms.

Chapter 4 contains the analysis of data and includes the discussion on the results obtained from the study.

Chapter 5 consists of broad conclusions drawn from this study.

Chapter-2 Site Amplification: A brief Review

2.1 Introduction

Since structures are built over a great variety of geological sites, it is important to measure the site amplification of ground motion throughout the metropolitan regions in earthquake prone zone areas. The site response parameters are used to distinguish regions where the seismic hazard is high due to amplification from the surface geology. The information about local site effects is also necessary for the simulation of realistic ground motion at the sites of interest. The most important methods developed so far to compute the site response consider either the S-wave or the Coda wave (Aki and Phillip, 1986). In this chapter various methods to compute site amplification characteristics have been discussed. The estimation of resonant frequencies of the near sub surface deposits at a site is an important aspect of a seismic microzonation project. The information of site response characteristics can be used for developing land-use plan for the urban regions and is very useful in the earthquake disaster mitigation.

2.2 Methods

A number of methods have been developed so far to estimate the site response. The empirical techniques can be divided into two categories viz., the reference site and non-reference site techniques. In the reference site technique, the concept states, the two sites that has similar source, path effects and reference site will have the flat spectrum response. The spectrum of the site of interest is divided by that of a nearby reference site situated on hard medium. This method is also termed as S-wave Spectral ratio method and depends on the availability of the reference site (one with negligible site response). The spectral ratio gives the estimate of site characteristics.

A rock site may not be available at all the times and hence, alternate techniques using non reference site have also been applied in the estimation of site response characteristics. In the non-reference site approach, the spectrum of the horizontal component is divided by that of vertical component recorded at the same site. A technique, based on microtremor, introduced by Nakamura (Nakamura, 1989) became popular because of its low cost and simple field operations. The most frequent empirical technique used for the site response estimation is the Spectral Ratio Method (Borcherdt, 1970) and the Coda Wave Spectral Ratio Method (Aki and Phillip, 1986). The well-established separatability of source, path and site effects on coda

waves of local seismic events provides the most effective way of estimating the site amplification effect. Because the structures are constructed over a large variety of geological sites, it is important to estimate the characteristics of site amplification of ground motion in the earthquake prone areas. To estimate the site amplification, it is necessary to remove the effect of source and path from the seismogram.

2.2.1 Horizontal to Vertical Spectral Ratio Method (HVSR)

The H/V spectral ratio is one of the most common approaches to evaluate local site effects. This method also called the "Nakamura technique". The basic assumption in this technique is that vertical component is not affected by local site geologic structure, whereas the horizontal components contain the P to S conversions induced by the local geology underlying the rock site.

Site response is obtained by deconvolving the vertical component from the horizontal component. In the frequency domain, this corresponds to the division of horizontal spectrum by the vertical spectrum (Castro et al., 1997).

The method allows the elimination of source and path effects by taking the spectral ratios of sample window when distance to reference site is small as compared to source to site distance. The resonant period and site amplification are determined by dividing the smoothened horizontal component by the smoothened vertical component of the spectrum, recorded at the same site. The two horizontal components are merged taking the root mean squared value,

$$H(f) = \sqrt{\frac{H(f)^2(EW) + H(f)^2(NS)}{2}} \quad (1)$$

Where, H(f)(EW) is the Fourier amplitude of S-wave window on the horizontal component in east- west direction, H(f)(NS) is the Fourier amplitude of S-wave window on the horizontal component in north-south direction and H(f) is the Fourier amplitude of the merged horizontal component of the event recorded at a station V(f) is the Fourier amplitude of the S-wave window on the vertical component for the event recorded at a station. Site amplification is taken to be the ratio of both components.

2.2.2 S-wave Spectral Ratio Method

This method involves computing the spectral ratio of the S-wave to the Coda wave at one station or the spectral ratio of horizontal to vertical component at a station to estimate site amplification. This method allows the elimination of source and path effects by taking the spectral ratios of sample window when distance to the reference site is small as compared to the source-to-site distance(Bonilla et al., 1997). The high frequency local earthquakes have been studied to estimate the local site amplification for various seismic regions.

A seismogram may be represented by a convolution of the source, path, site and instrument response and is given as:

$$A_{ij}(f)=S_i(f)P_{ij}(f)G_j(f)I_j(f) \quad (2)$$

where, 'i' is the event and 'j' is the station.

S_i (f) - source term for i_{th} event,

P_{ij} (f) - path term for i_{th} event and j_{th} station

G_j (f) - the site term for j_{th} station, and

I_j (f) - instrument response term for j_{th} station.

After removing the instrument response for each station, the spectral ratio is obtained by dividing the Fourier spectrum of the acceleration for the S wave at the j_{th} station by the spectrum of the S wave at the k_{th} reference station (Bonilla et al. 1997)

$$\frac{Aij(f)}{Aik(f)} = \frac{Si(f)Pij(f)Gj(f)}{Si(f)Pik(f)Gk(f)} \quad (3)$$

The source term may not necessarily be the same for j_{th} and k_{th} stations because of focal mechanism and directivity effects, however, by using a large number of such events these effects are averaged out. Thus equation 2 can be written as:

$$\frac{Aij(f)}{Aik(f)} = \frac{Pij(f)Gj(f)}{Pik(f)Gk(f)} \quad (4)$$

Path term can be assumed same for two stations if the separation between the two staions is less than the hypocentral distances then (Bonilla et al. 1997). Each spectra at j_{th} station for the i_{th} event is multiplied by a correction factor. Therefore equation 3 can be rewritten as:

$$\frac{Aij(f)}{Aik(f)} = \frac{Tij(f)Gj(f)}{Tij(f)Gk(f)} \quad (5)$$

Thus the amplification or deamplification is obtained at j_{th} station for the i_{th} event relative to a reference site. The reference site is so choosen that it has the advantage of recording nearly all the events making direct spectral ratios possible and should be located on hard rock.

2.3 Literature Review

Various attempts has been made in the past to study the site amplification characteristics using S-wave, Coda wave and H/V spectral ratio method. Also the comparison has also been addressed in number of studies.

1) Bonilla et al. (1997) have estimated site amplification in San Fernando Valley using S-wave, Coda wave and H/V spectral ratio. Study shows that H/V method is capable of revealing the predominant frequency peaks but their amplification values are different from the values determined from S-wave and Coda wave method.
2) Borcherdt (1970) have estimated site amplification of horizontal and vertical components of S-waves generated due nuclear explosions near San Francisco Bay relative to a bed rock site. Study shows that the amplification of both components differ based on the nature of the soil.
3) Castro et al. (1997) have estimated the site amplification of S-wave site response using H/V Spectral ratio method using the data of Friuli earthquake, Italy (1976). Study shows that the resulting site functions shows small amplifications for most of the sites within a factor of 2 and the high amplification obtained at some station are results of contamination of Rayleigh waves.
4) Chopra et al. (2012) have estimated the site amplification due to Bhuj earthquakes Gujarat using H/V spectral ratio method. Study shows the spatial variation of predominant frequencies and their corresponding site amplification. The resulting amplifications was of the order of 5.
5) Sudhakar. A. (2012). The site amplification characteristics from S-wave and HVSR method were computed at 12-station seismological network deployed in the Garhwal Lesser Himalaya region were obtained using the microtremer data for HVSR method.

Chapter-3 Data Analysis

3.1 Introduction

A 12 station local seismological network has been deployed in the environs of Tehri in the Garhwal Himalaya by the Department of Earthquake Engineering, IIT Roorkee for continuously monitoring the local seismicity of the region around a dam site. This study uses the digitally recorded data of three components of six earthquakes recorded at 12 stations of the network. The various aspects such as seismological network, selection of events, rotation of horizontal components into radial and transverse and analysis of data to compute the site response are discussed in this Chapter.

3.2 Data Used

The present study is based on the analysis of 201 waveforms from six local earthquakes recorded during the year 2012-2017 in the Garhwal Himalaya region for H/V spectral ratio method and 114 seismograms from four local earthquakes for S-wave spectral ratio method. The data of six local earthquakes has been collected from the 12 station seismological network under operation around Tehri region in the Garhwal Lesser Himalaya. This network is being operated by the Department of Earthquake Engineering, IIT Roorkee and the study is sponsored by the Tehri Hydro Development Corporation India Limited (THDC). The geographical coordinates and other details including rock types at 12 stations and one station at Roorkee are given in Table 3.1. The three component digital data of all the events at 12 stations is recorded by a triaxial short-period seismometer (CMG 40T-1, frequency range: 1 Hz — 100 Hz) coupled to a 24-bit data acquisition system (DAS 130-01/03). The data is measured at every station at a rate of 100 samples /second /component. The hypocenter parameters namely latitude, longitude, focal depth and origin time are estimated using HYPO -71 PC programme (EQ: 2011-26. The matrix of six events used for estimation of site amplification using HVSR and four events used for the site amplification using S-wave spectral ratio method are shown in Table 3.2 and Table 3.3. The epicentral locations of these events are shown in the tectonic map of the area in Figure 3.1. All the local events are recorded in the epicentral distance within the range of about 200 km having focal depth range of 4.4 km to 40 km and magnitudes of these events fall in the range from ML 3.9 to ML 5.

Figure 3.2 shows an example of three component records at 12 stations of an event occurred on 22-08-2017 in the region.

Table 3.1: Recording stations detail of the network.

No.	Station	Code	Location		Type of rock	Elevation (m)
			Lat. (ºN)	Long(ºE)		
1.	Ayarchali	AYAR	30.303	78.431	Sandstone	2106
2.	Chandrabadni	CHAN	30.305	78.619	Phyllites	2244
3.	Chintarbagi	CHIN	30.409	78.454	Phyllites	1953
4.	Giyanja	GIYA	30.755	78.421	Sandstone	2113
5.	Khurmola	KHUR	30.580	78.495	Sandstone	1730
6.	New Tehri	NEWT	30.376	78.429	Slates	1914
7.	Pratapnagar	PRAT	30.458	78.475	Quartzite	2128
8.	Rajgadi	RAJG	30.844	78.238	Sandstone	1908
9.	Sirala	SIRA	30.132	78.633	Sandstone	1424
10.	Srikot	SRIK	30.612	78.299	Phyllites	1617
11.	Surkanda Devi	SURK	30.410	78.289	sandstone	2754
12.	Vinakkhal	VINA	30.553	78.655	Phyllites	1640

Table 3.2: Hypocentre parameters of the events used in HVSR.

No.	Date	Origin Time Hr:Mn:Sec	Geographical coordinates Lat. (ºN)	Long. (ºE)	Depth (Km)	Magnitude (M_L)
1	28-07-2012	05:48:06	29.760	80.506	11.9	4.7
2	11-02-2013	10:48:52	30.877	78.324	38.4	4.0
3	09-10-2014	01:14:29	30.200	80.407	9.8	3.7
4	18-07-2015	23:48:09	30.508	79.047	15.0	4.1
5	01-12-2016	16:52:51	29.877	80.287	17.0	4.9
6	22-08-2017	15:22:05	30.510	79.530	4.4	3.7

Table 3.3: Hypocentre parameters of the events used in S-Wave Spectral Ratio Method.

No.	Date	Origin Time Hr:Mn:Sec	Geographical coordinates Lat. (ºN)	Long. (ºE)	Depth (Km)	Magnitude (M_L)
1	28-07-2012	05:48:32	29.760	80.506	11.9	4.7
2	11-02-2013	10:48:52	30.877	78.324	38.4	4.0
3	18-07-2015	23:48:09	30.508	79.047	15.0	4.1
4	01-12-2016	16:52:51	29.877	80.287	17.0	4.9

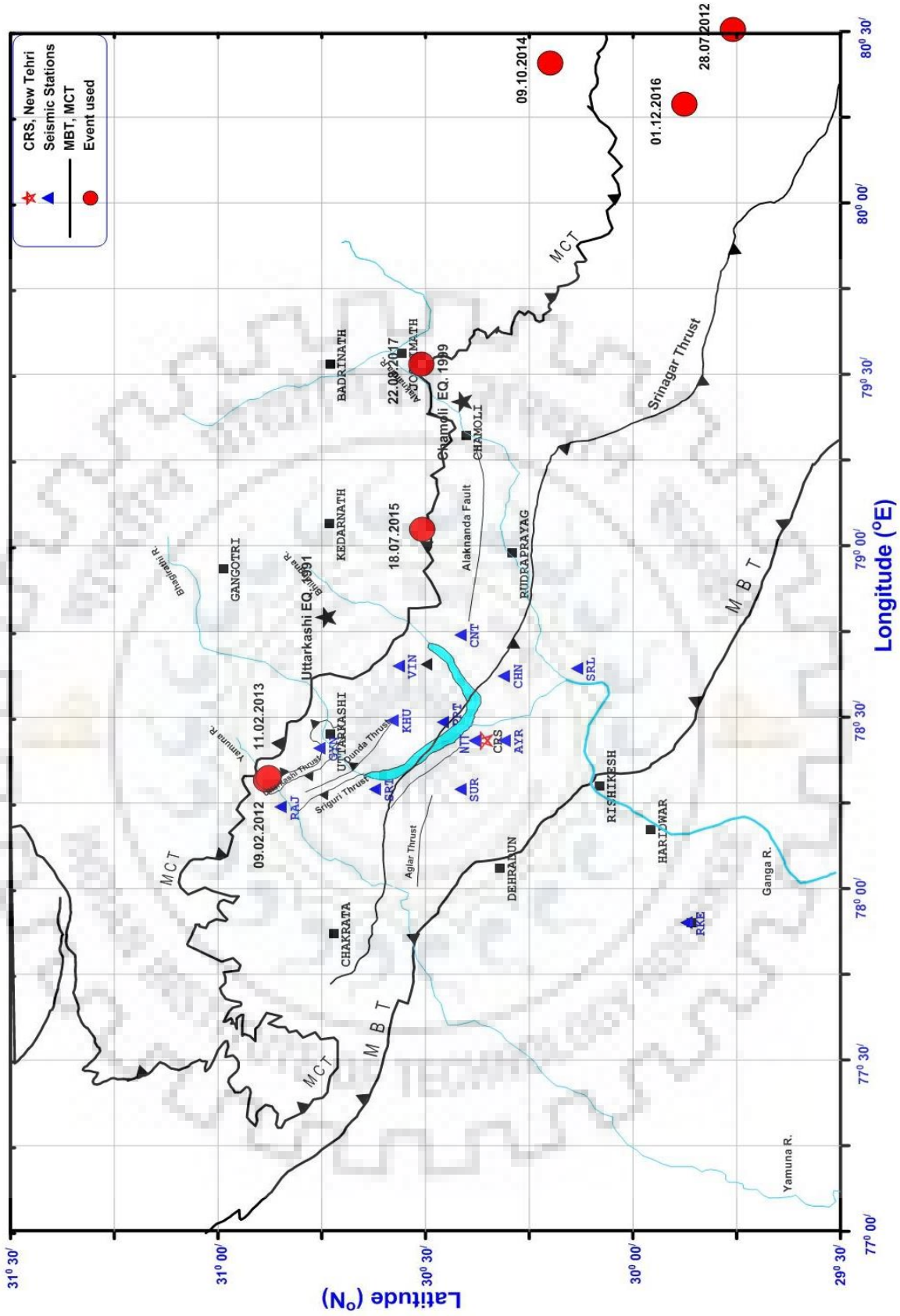

Figure 3.1: Map showing location of events used.

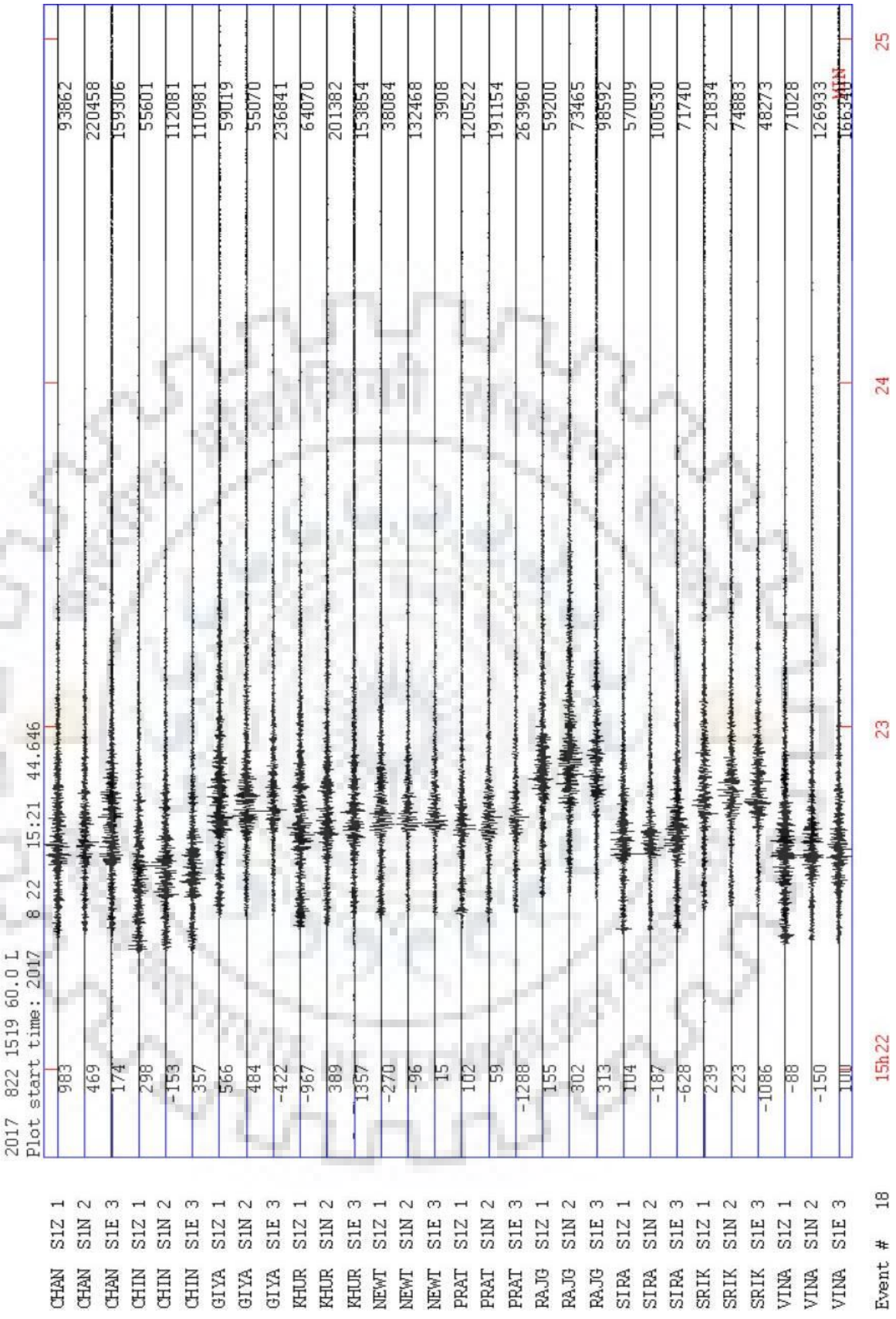

Figure 3.2: An example of three component record at 12 stations of an event recorded on 22/08/2017 in the region.

3.3 Data analysis by H/V spectral ratio method

Estimation of the site amplification factors from the analysis of seismograms recorded digitally. A time window is selected that contains prominent part of the seismogram to compute the Fourier spectrum.

Following is the procedure adopted for the analysis of digitally recorded seismograms. A station records two horizontal components viz. North-South component and East-West component, and one vertical component of an earthquake.

The instrument correction has been applied to the recorded data. Fast Fourier Transform (FFT) function is used to compute the Fourier amplitudes of the spectra records of each station-event pair, and analysed independently. The onset time of noise on the seismograms are determined visually. The two horizontal components are merged taking the root mean square of the values. The H/V vs frequency curves were obtained for all the stations and these curves are studied to obtain the predominant frequency of the soil. The Fourier amplitudes of HVSR were centered over frequency bands from 1 Hz to 12 Hz respectively to obtain the amplitude estimations at different frequencies.

3.4 Data Analysis by S-wave spectral ratio method

Estimation of the site amplification factors from the analysis of seismograms recorded digitally at stations is done using a time window having prominent part of the S-wave. The selected S-wave part has been used to compute the Fourier spectra.

Following is the procedure adopted for the analysis of digitally recorded seismograms. Different kinds of seismic waves have their particle motion or the amplitude in different directions. The analysis of the particle motion is used to identify the different wave types. The particle motion or polarization of the waves is best looked at in a coordinate system, that points from the earthquake epicenter to the seismic station. The two horizontal components are rotated into the radial (R) and transverse (T) components by a simple rotation. The radial direction is along the line from the station to the event and the transverse direction is in the horizontal plane at a right angle to the radial direction.

The rotation is computed using

$$\text{Radial} = -\text{NS}\cos(\varphi) - \text{EW}\sin(\varphi) \quad (6)$$

$$\text{Transverse} = \text{NS}\sin(\varphi) - \text{EW}\cos(\varphi) \quad (7)$$

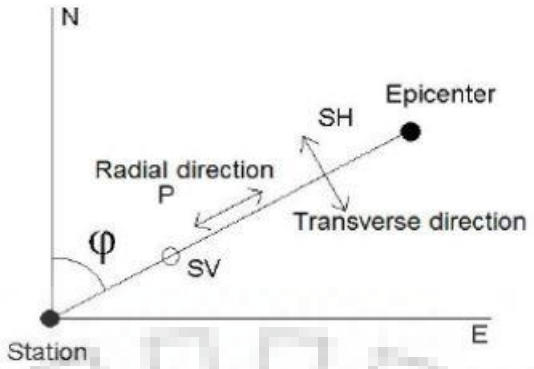

Figure 3.3: Definition of radial and transverse direction *(Sudhakar, 2012).*

Where, φ is the back azimuth angle, defined as the angle between the north and the radial direction. (Figure 3.3) Radial, Transverse, EW and NS are the amplitudes in respective directions. The two components viz. east-west and north-south were rotated with respect to their azimuth from the epicentre by using the equations 6 & 7 into radial and transverse direction. Before rotating horizontal components corrections such as base line and the instrument corrections were applied to the data

The instrument correction has been applied to all the records, and then the Fast Fourier Transform (FFT) function is used to obtain the Fourier amplitudes of S waves for the records of each station and event pair, and analysed separately. Visual determination is done for the onset of S-wave on the seismograms. One-time window of the recorded seismograms has been used for the calculation of the Fourier spectrum. The Fourier amplitudes of S-wave were obtained over the frequency bands range 1.0 Hz to 12.0 Hz. Calculation of spectral ratios of each component has been done with respect to the reference station at every station.

Chapter-4 Results

4.1 Introduction

The time series of s-waves, from six local earthquakes, comprises 201 seismograms and 114 seismograms of four local earthquakes have been analysed to estimate H/V spectral ratio and S-wave spectral ratio respectively. These earthquakes span the epicentral distance upto 200 km, focal depth range from 4 km to 40 km and local magnitude range from 3.5 to 5.0. Two methods have been adopted to estimate the site amplification factors, S-wave spectral ratio and H/V spectral ratio method. The data has been analysed in the frequency range from 1 Hz to 12 Hz to estimate the site amplification factors using the S-wave spectral ratio method and from 1 Hz to 12 Hz for H/V ratio method. The results obtained on the estimated site amplification factors using S-waves and H/V method at 12 recording sites located in the Garhwal Himalaya region are discussed in this Chapter.

4.2 Site amplification from H/V spectral ratio method

The frequency range and amplification value at the predominant frequency are obtained from the HVSR curves for all the six events considered in the analysis. To permit computing H/V ratios, the root mean squared resultant of two horizontal components has been divided by the vertical component. Tables 4.1, 4.2, 4.3, 4.4, 4.5, 4.6, 4.7 shows the amplification factors corresponding to frequency. The amplification peaks for all the six events occured in the frequency ranging from 2 Hz to 5 Hz at 11 sites, whereas at CHAN these peaks has been observed in the range 5 Hz to 10 Hz. The natural resonant frequency at each site is considered as the first peak of the event at the site.

Figure 4.1 shows the response of H/V spectral ratio of the event recorded by the network on 28 July 2012. For each site about 180 seconds of data sample collected for the earthquake of magnitude (Mw= 4.7) has been analysed and interpreted. The maximum amplification factors of six times has been observed at GIYA, KHUR and PRAT sites with prominent peak between 1 Hz and 4 Hz. The response at AYAR, NEWT, RAJG, SIRK and SURK site are almost similar with an amplification factor of four in the frequency ranging from 1 Hz to 4 Hz. For CHIN and SURA site, the amplification is almost 2 times with no prominent peak.

Figure 4.2 shows the response of H/V spectral ratio of the event recorded by the network on 11 Feb 2013. For each site about 180 seconds of data sample collected for the earthquake of magnitude (Mw= 4.0) is analysed and interpreted. A maximum amplification of 10 times at the frequency range from 7 Hz to 10 Hz has been obtained at CHAN site. AYAR, GIYA, and KHUR sites show the amplification value of six in the frequency range 2 Hz to 4 Hz. NEWT, PRAT and RAJG site show amplification of five times in frequency range 1 Hz to 3 Hz while other sites show low amplification.

Figure 4.3 shows the response of H/V spectral ratio of the event recorded by the network on 09 Oct 2014. For each site about 180 seconds of data sample collected for the earthquake of magnitude (Mw= 4.0) is analysed and interpreted. At all sites, amplification peaks have been observed at frequency ranging from 2 Hz to 5 Hz. The response has almost uniform level of amplification of the order between two and three for RAJG, SIRA, SIRK, SURK and VINA sites. Lesser amplification has been observed at CHIN site. AYAR, GIYA, KHUR and PRAT site show high amplification factor in frequency range 2 Hz to 4 Hz.

Figure 4.4 shows the response of H/V spectral ratio of the event recorded by the network on 18 July 2015. For each site about 180 seconds of data sample collected for the earthquake of magnitude (Mw= 4.1) is analysed and interpreted. Maximum amplification is observed at KHUR sites of 7 times at a frequency ranging from 2 Hz to 4 Hz. The dominant peaks are observed between 2Hz to 4 Hz for other sites. GIYA, NEWT, PRAT and SIRK has amplification of around four times. AYAR, CHIN, RAJG, SIRA and SURK and VINA sites have amplification factor of three. CHAN site have negligible amplification.

Figure 4.5 shows the response of H/V spectral ratio of the event recorded by the network on 01 Dec 2016. For each site about 180 seconds of data sample collected for the earthquake of magnitude (Mw= 4.9) is analysed and interpreted. Maximum response is obtained at GIYA and KHUR sites of six times at a frequency ranging from 2 Hz to 4 Hz. The dominant frequency peaks are observed between 2Hz to 4 Hz for all other sites except at CHAN site. PRAT, SIRK and SURK sites has amplification of around four times. AYAR, RAJG and VINA sites have amplification factor of three. NEWT site have negligible amplification.

Figure 4.6 shows the response of H/V spectral ratio of the event recorded by the network on 22 Aug 2017. For each site about 180 seconds of data sample collected for the earthquake of

magnitude (Mw= 3.7) is analysed and interpreted. Maximum amplification has been obtained at GIYA site of seven times at a frequency ranging from 1 Hz to 2 Hz. AYAR, CHIN and RAJG has maximum amplification of three in frequency range 3 Hz- 5 Hz. NEWT and PRAT has amplification value of the order of four. CHAN site has maximum amplification at a frequency ranging 6 Hz to 9 Hz. SIRA site has lesser amplification.

Figure 4.7 shows the response of H/V spectral ratio of the average of six events recorded by the network. GIYA and KHUR sites shows higher amplification of the order of six compared to other sites at a frequency ranging from 2 Hz- 5 Hz. AYAR and PRAT has amplification of four while other sites have low amplification of two.

4.3 Site Amplification from S-wave spectral ratio method

Site amplification estimated from four events located around centre of the network have been discussed separately with PRAT as reference station. Table 4.8, 4.9, 4.10 and 4.11, Figures 4.8, 4.9, 4.10 and 4.11 show S-wave site amplification factors of the radial, transverse and vertical components for all the sites relative to PRAT. Each factor was determined independently for each component.

Figure 4.8 shows the amplification estimates for the three components at 6 sites with PRAT site as reference site for event occurring south-east of the network on 28 July 2012 AYAR, CHIN and KHUR sites show similar trends with maximum site amplification of 6 at frequency between 4Hz to 6 Hz. Maximum amplification of 6 times has been obtained at CHIN site at a frequency of 5 Hz. This is due to location of the site, located at a height of 2244 m. Lesser site amplification has been brought out at CHAN site. RAJG site shows increase in amplification with frequency. Vertical component shows the lowest amplification at all sites.

Figure 4.9 shows the site amplification for the three components at 11 sites with PRAT site as reference site for event occurring north-west of the network on 11 Feb 2013. Similar frequency trend in the amplification has been obtained in the radial and transverse components. Radial and vertical components at AYAR, CHIN, KHUR, NEWT sites shows amplification of 3 times at low frequencies between 2 Hz and 4 Hz. High amplification of 6 times in the transverse component is obtained at frequency 8 Hz at CHAN, GIYA and RAJG

sites. At sites SIRK and VINA maximum amplification is obtained at frequency 8 Hz of 4 and 3 times respectively. Lesser amplification has been obtained at SURK and SIRA sites.

Fig 4.10 shows the site amplification for the three components at 11 sites with PRAT site as reference for the event taking place north-east of the network on 18 July 2015. Majority of sites shows similar frequency-amplification trend in the radial and transverse components. Maximum site amplification of 6 times has been obtained at AYAR and SIRA site at a frequency 7 Hz and 5 Hz respectively. NEWT, RAJG and VINA shows peak at a frequency of around 9 Hz of order three. SURK and KHUR sites shows amplification of order four between frequency 2 Hz to 5 Hz. Less amplification has been observed at CHAN site.

Fig 4.11 shows the site amplification for the three components at 11 sites with PRAT site as reference site for the events occurring to the southeast of the network on 01 Dec 2016. Almost similar frequency dependent trends have been observed at CHAN and SIRA site having maximum amplification near frequency of 10 Hz of the order 8 and 6 respectively. This high site amplification is due to the location of the site located at a height of 2244 m. The pattern of site amplification observed at AYAR, GIYA, RAJG and SURK sites are almost similar. Low amplification has been obtained at NEWT, SIRK site.

Table 4.1 HVSR amplification for earthquake 28-07-2012.

FREQUENCY	1	2	3	4	5	6	7	8	9	10	11	12
AYAR	1.79	3.45	3.75	2.71	3.15	1.51	1.50	1.80	1.88	1.92	1.69	1.45
CHIN	0.93	1.24	1.52	1.97	2.32	2.45	1.72	1.64	1.37	1.22	1.39	1.65
GIYA	2.89	5.73	2.69	1.63	0.70	0.97	1.56	1.73	1.63	1.56	1.17	1.03
KHUR	2.54	3.66	4.67	4.23	2.59	1.91	1.31	1.11	1.36	1.43	1.58	1.88
NEWT	2.17	3.73	3.40	2.10	1.86	2.02	1.63	1.72	1.31	1.13	1.27	1.64
PRAT	4.28	2.99	3.07	2.15	1.33	1.37	0.95	0.86	1.10	1.33	1.14	1.16
RAJG	3.28	2.46	1.58	1.21	1.59	2.08	1.86	1.60	1.60	1.61	1.55	1.60
SIRA	1.23	1.31	1.57	1.48	1.61	1.87	1.76	1.59	1.33	1.10	1.00	0.96
SIRK	2.48	1.71	1.87	1.35	1.10	1.62	1.51	1.85	1.39	1.23	1.22	1.31
SURK	1.67	1.02	3.79	2.25	1.56	1.40	1.28	1.49	1.64	1.66	1.59	1.36

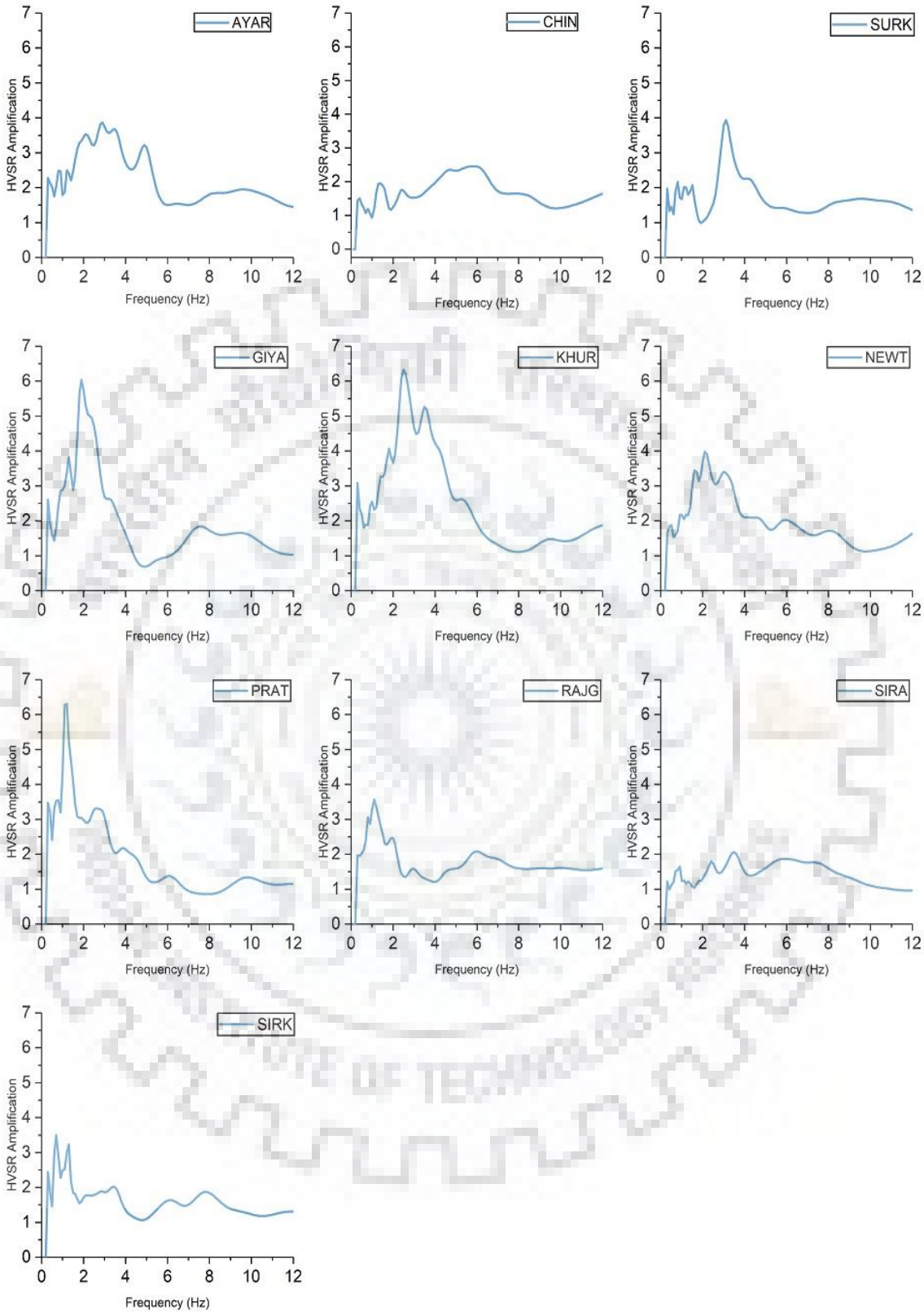

Figure 4.1: Site amplification for 28-07-2012 earthquake.

Table 4.2: HVSR amplification for earthquake 11-02-2012.

FREQUENCY	1	2	3	4	5	6	7	8	9	10	11	12
AYAR	1.30	2.36	4.89	4.24	2.99	1.35	1.58	1.99	1.90	1.78	1.76	1.66
CHAN	3.51	7.17	5.61	6.05	7.49	7.19	8.92	8.64	6.41	4.84	4.00	3.66
CHIN	1.23	2.38	1.48	2.09	1.90	1.72	1.73	1.55	1.49	1.21	1.15	1.16
GIYA	2.61	4.96	5.78	2.40	1.15	2.10	2.64	3.00	3.53	2.95	2.66	2.86
KHUR	2.71	4.50	6.17	2.79	2.00	1.33	1.08	1.07	1.17	1.33	1.26	1.29
NEWT	2.59	4.87	1.96	1.24	1.52	1.58	1.43	1.00	0.78	0.85	0.92	1.02
PRAT	2.77	2.65	2.97	2.78	2.27	1.12	1.04	1.19	1.38	1.21	1.17	0.99
RAJG	3.57	3.20	1.15	1.07	1.52	1.69	1.21	1.50	2.01	1.90	1.51	1.43
SIRA	0.83	0.87	1.36	2.01	1.39	1.88	1.38	1.32	1.85	1.79	1.42	1.24
SIRK	2.19	2.77	1.89	2.82	1.96	1.16	0.93	1.20	1.64	1.81	1.69	1.51
SURK	1.16	1.18	1.13	1.20	1.46	1.40	1.45	1.15	1.14	1.17	1.15	1.31
VINA	2.26	2.41	2.13	2.60	1.40	1.78	1.30	1.14	1.51	1.41	1.57	1.35

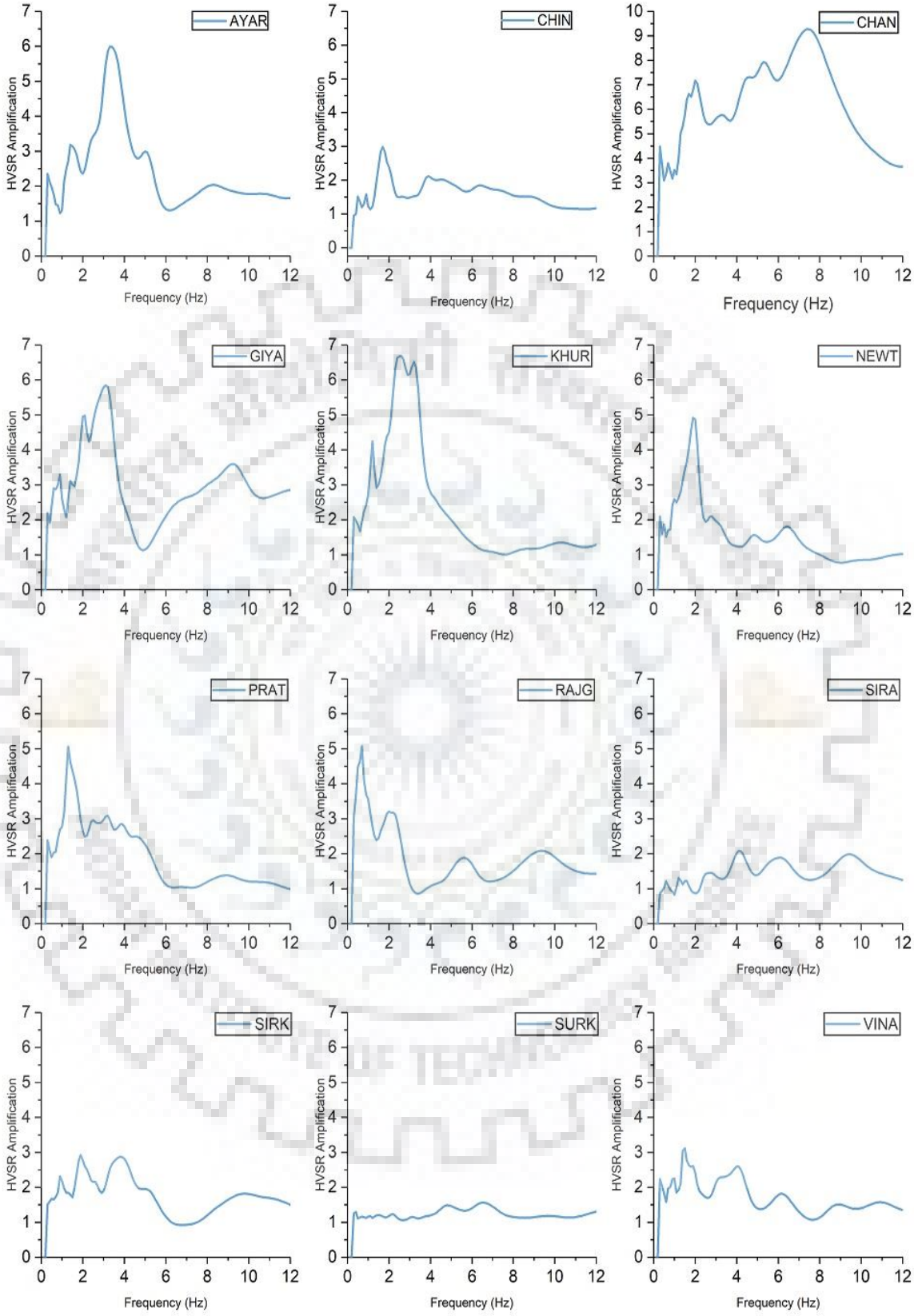

Figure 4.2: Site amplification for 11-02-2013 earthquake.

Table 4.3: HVSR amplification for earthquake 09-10-2014

FREQUENCY	1	2	3	4	5	6	7	8	9	10	11	12
AYAR	3.36	3.14	1.99	4.58	1.88	1.02	0.75	0.97	1.58	1.64	1.41	1.45
CHIN	0.01	0.00	0.00	0.00	0.00	0.00	0.01	0.01	0.01	0.01	0.01	0.02
GIYA	3.01	5.99	4.80	1.44	0.73	0.91	1.63	1.69	1.41	1.28	1.18	1.20
KHUR	3.01	4.96	6.41	3.89	2.87	2.30	1.95	1.76	1.87	2.42	2.54	2.53
NEWT	2.92	4.35	2.28	2.47	2.59	1.98	1.86	1.34	1.34	1.53	1.81	1.87
PRAT	3.74	3.24	1.74	1.85	1.51	1.10	0.94	0.83	0.90	0.98	1.04	1.20
RAJG	2.38	1.40	1.89	2.16	1.43	1.51	1.54	1.44	1.60	1.48	1.61	1.66
SIRA	1.26	1.07	1.74	1.19	1.33	1.50	1.62	1.70	1.38	1.09	0.99	1.04
SIRK	2.04	1.17	2.02	1.94	1.08	1.28	2.02	1.26	1.09	1.18	1.21	1.18
SURK	2.56	2.46	2.84	1.50	1.64	1.69	1.38	1.21	1.28	1.33	1.41	1.59
VINA	1.66	1.73	2.77	1.54	1.34	1.56	1.78	1.70	1.30	1.30	1.28	1.24

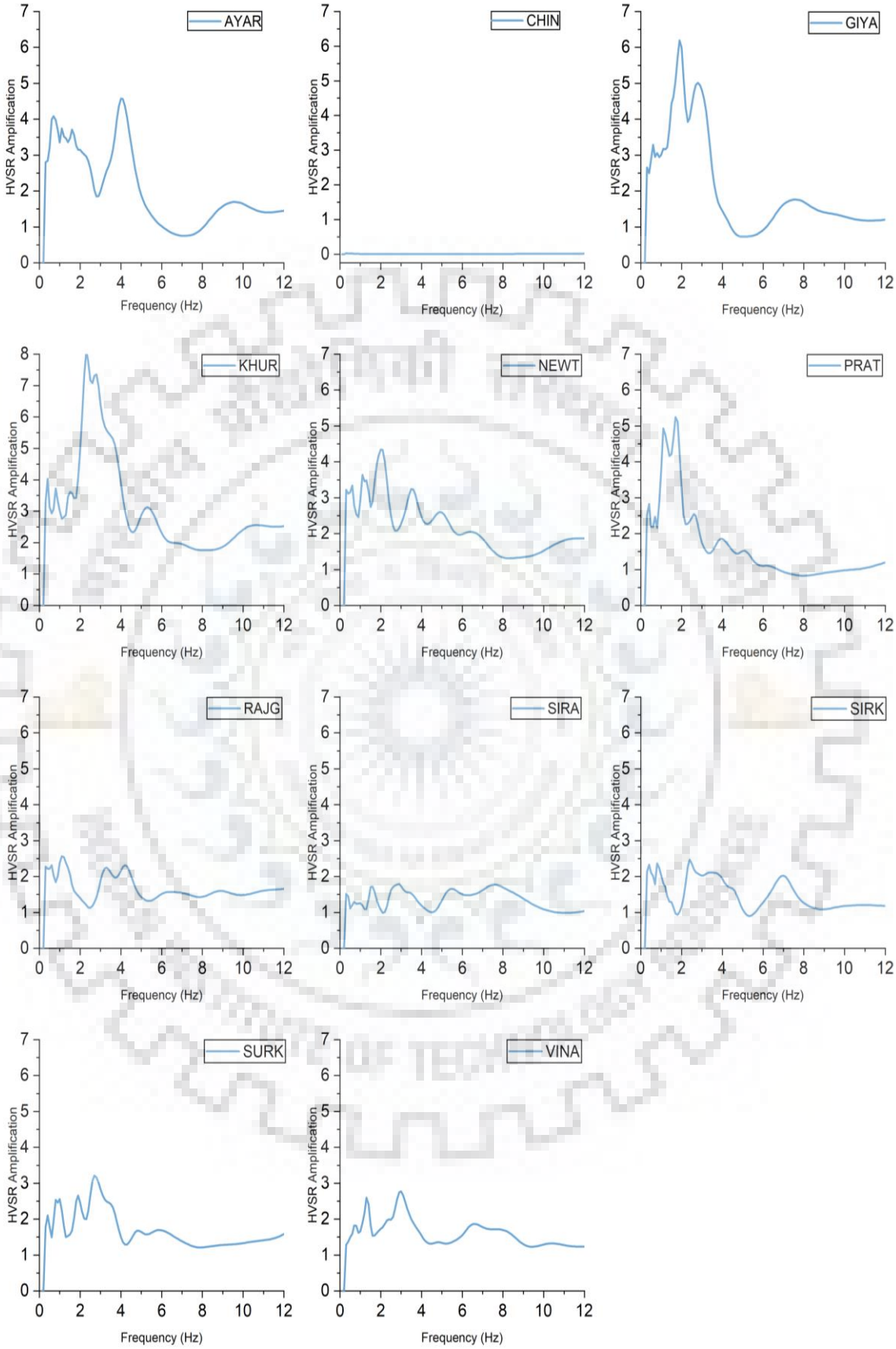

Figure 4.3: Site amplification for 09-10-2014 earthquake.

Table 4.4: HVSR amplification for earthquake 18-07-2015.

FREQUENCY	1	2	3	4	5	6	7	8	9	10	11	12
AYAR	2.49	2.84	2.57	2.31	2.61	1.25	0.98	1.36	1.68	1.76	1.65	1.76
CHAN	0.03	0.04	0.03	0.03	0.03	0.05	0.04	0.06	0.05	0.03	0.02	0.02
CHIN	1.47	1.46	2.45	2.58	1.97	2.62	1.78	1.77	1.38	1.33	1.50	1.50
GIYA	1.57	3.61	2.62	2.06	0.82	1.30	1.87	1.80	1.48	1.04	1.03	1.16
KHUR	3.39	4.14	7.29	3.50	2.36	1.60	0.91	1.02	1.18	1.32	1.35	1.38
NEWT	3.05	2.79	2.75	2.56	2.18	2.57	1.39	1.00	0.99	0.83	1.02	1.22
PRAT	3.84	3.80	2.32	2.48	2.05	1.52	1.24	1.55	1.58	1.14	0.95	1.01
RAJG	1.27	1.04	1.94	1.33	1.55	2.07	2.05	1.83	1.56	1.88	1.61	1.47
SIRA	1.04	1.01	1.19	1.91	1.66	1.34	1.09	1.07	1.00	0.95	0.94	0.85
SIRK	2.68	3.03	3.81	2.69	1.95	1.92	2.01	1.88	2.22	2.12	1.67	1.51
SURK	0.92	1.56	1.64	1.39	1.49	1.64	1.62	1.58	1.41	1.67	1.66	1.26
VINA	1.94	2.56	2.60	1.20	1.68	2.31	1.71	1.72	1.77	1.46	1.45	1.28

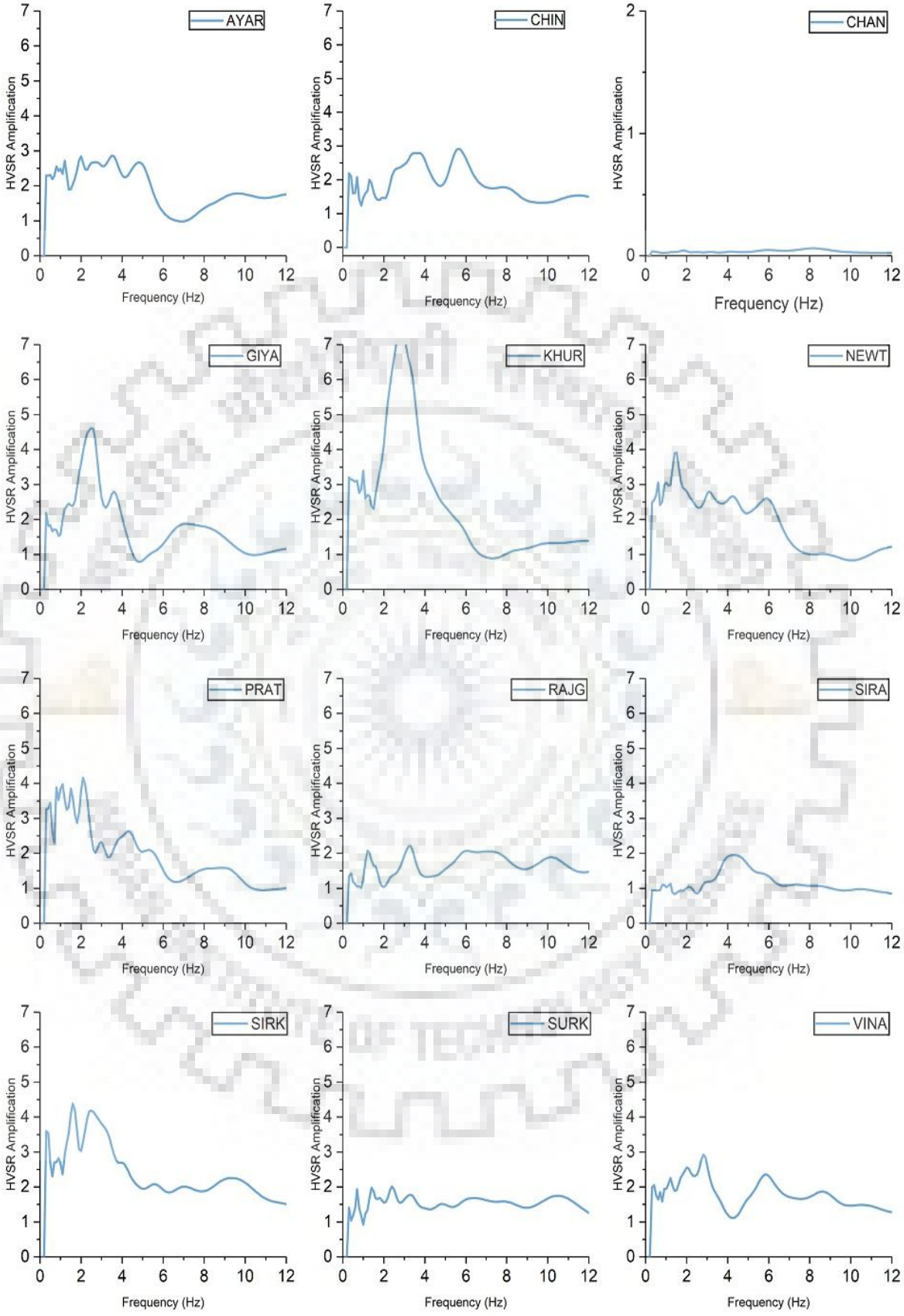

Figure 4.4: Site amplification for 18-07-2015 earthquake.

Table 4.5: HVSR amplification for earthquake 07-12-2016.

FREQUENCY	1	2	3	4	5	6	7	8	9	10	11	12
AYAR	2.60	2.73	2.50	2.45	2.26	1.39	1.18	1.13	1.35	1.51	1.28	1.13
CHAN	1.50	1.11	1.86	2.00	2.27	3.35	3.74	2.35	2.15	1.91	1.61	1.46
CHIN	1.67	2.46	4.98	2.28	2.62	2.73	1.75	1.45	1.23	1.33	1.29	1.23
GIYA	2.25	5.65	4.39	1.53	0.77	0.79	1.27	1.59	1.88	2.07	1.79	1.65
KHUR	2.74	3.20	6.09	3.40	3.10	1.93	1.29	1.17	1.06	1.41	1.91	2.10
NEWT	0.30	0.44	0.42	0.30	0.38	0.26	0.23	0.20	0.21	0.21	0.19	0.21
PRAT	2.69	3.05	2.47	3.52	1.73	1.22	1.17	1.27	1.09	1.39	1.42	1.35
RAJG	2.10	3.01	1.29	1.35	0.98	1.27	1.38	1.30	1.30	1.08	0.95	1.11
SIRA	0.92	1.36	1.73	1.45	1.77	1.57	1.56	1.42	1.00	0.95	1.05	1.12
SIRK	2.38	3.02	4.72	4.24	3.48	2.32	2.36	2.16	2.52	3.10	2.86	2.01
SURK	4.36	2.87	2.86	2.26	3.07	2.29	1.75	1.81	2.09	2.01	1.99	2.09
VINA	1.70	1.14	3.47	1.95	1.98	1.58	1.47	1.74	1.54	1.42	1.26	1.27

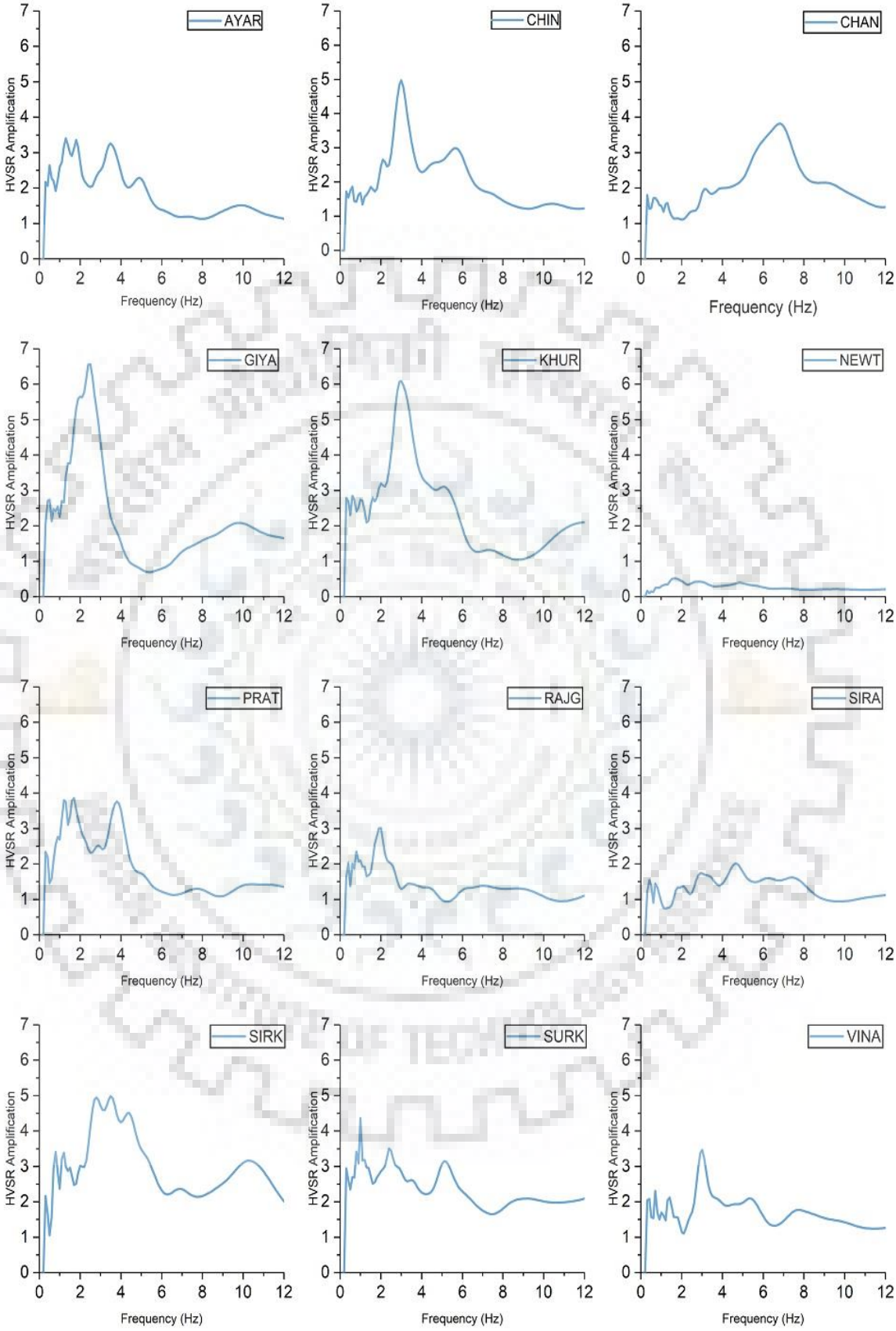

Figure 4.5: Site amplification for 01-12-2016 earthquake.

Table 4.6: HVSR amplification for earthquake 22-08-2017.

FREQUENCY	1	2	3	4	5	6	7	8	9	10	11	12
AYAR	1.69	2.94	2.34	3.67	1.99	1.18	1.22	0.97	1.43	1.50	1.28	1.29
CHAN	1.46	1.89	1.13	1.52	2.06	2.99	2.19	3.01	2.68	2.16	1.75	1.52
CHIN	2.06	1.65	3.11	3.23	2.69	1.69	1.85	1.44	1.23	1.15	1.34	1.50
GIYA	2.21	5.56	4.82	1.70	1.12	0.88	1.28	1.90	1.89	1.65	1.22	1.12
NEWT	2.74	3.05	4.55	1.79	1.28	1.49	1.57	1.47	1.27	1.05	1.11	1.26
PRAT	2.77	3.01	1.79	1.64	1.94	1.09	1.39	1.33	0.87	0.77	0.90	1.02
RAJG	2.16	2.51	1.48	1.40	1.49	1.54	1.36	1.63	1.41	1.16	1.21	1.23
SIRA	0.91	1.23	1.67	1.43	1.38	1.46	1.52	1.32	1.07	0.92	0.88	0.91
SIRK	2.61	4.67	4.60	2.70	2.55	2.36	2.27	2.24	2.26	2.15	2.04	1.96

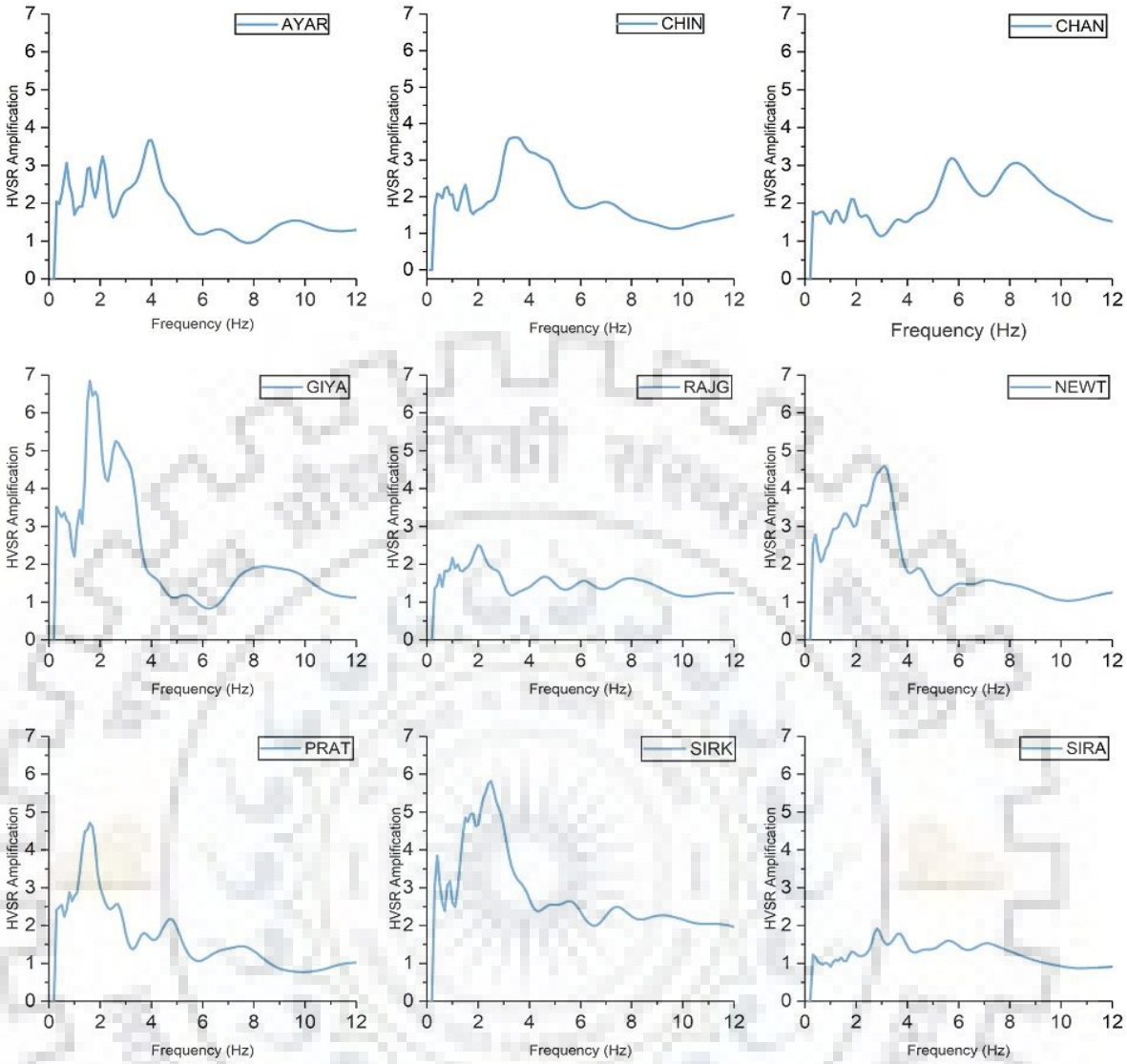

Figure 4.6: Site amplification for 22-08-2017 earthquake.

Table 4.7: HVSR amplification for average of earthquakes.

FREQUENCY	1	2	3	4	5	6	7	8	9	10	11	12
AYAR	2.10	2.89	2.86	3.21	2.43	1.27	1.17	1.32	1.62	1.68	1.50	1.44
CHAN	0.69	1.14	1.22	1.59	2.07	2.53	2.50	2.47	1.98	1.47	1.18	1.03
CHIN	0.58	0.60	0.81	0.78	0.74	0.75	0.68	0.64	0.58	0.58	0.62	0.66
GIYA	2.32	5.23	3.73	1.66	0.82	0.96	1.51	1.74	1.64	1.48	1.25	1.22
KHUR	2.87	4.04	6.06	3.53	2.55	1.78	1.27	1.20	1.30	1.54	1.67	1.78
NEWT	1.86	2.58	2.08	1.44	1.41	1.36	1.14	0.94	0.84	0.80	0.88	1.00
PRAT	3.29	3.11	2.34	2.33	1.78	1.23	1.11	1.14	1.13	1.11	1.09	1.11
RAJG	2.33	2.11	1.53	1.38	1.41	1.67	1.54	1.54	1.56	1.48	1.38	1.40
SIRA	1.02	1.13	1.53	1.55	1.51	1.59	1.47	1.39	1.24	1.10	1.03	1.01
SIRK	2.38	2.49	2.90	2.47	1.85	1.71	1.77	1.72	1.78	1.83	1.70	1.55
SURK	1.82	1.68	2.25	1.66	1.77	1.66	1.49	1.43	1.48	1.54	1.53	1.49
VINA	1.88	1.87	2.70	1.75	1.58	1.78	1.55	1.55	1.52	1.40	1.38	1.28

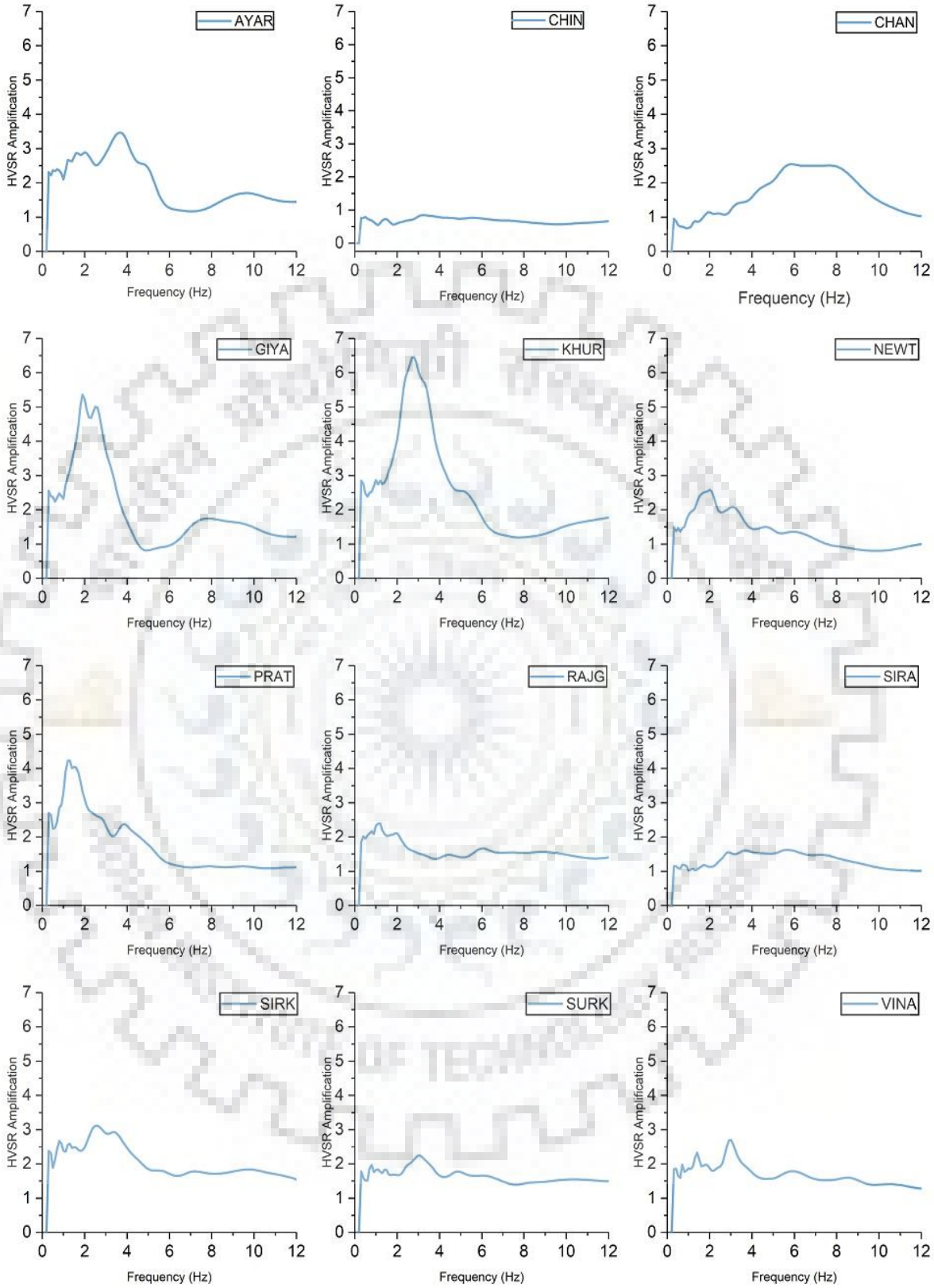

Figure 4.7: Site amplification for average of earthquakes.

Table 4.8: S-wave spectral ratio amplification for earthquake occurred south-east of PRAT on 28-07-2012 relative to PRAT station.

FREQUENCY		1	2	3	4	5	5	6	7	8	10	11	12
	RADIAL	0.12	0.22	0.15	0.24	0.32	4.29	0.98	2.06	2.94	0.94	2.34	2.04
AYAR	TRANSVERSE	0.04	0.06	0.76	0.54	1.37	7.43	0.56	1.50	1.69	1.69	1.40	1.56
	VERTICAL	1.04	0.22	0.70	0.70	0.11	2.59	1.98	2.72	0.55	0.41	2.09	0.51
	RADIAL	0.00	0.00	0.00	0.01	0.01	0.11	0.04	0.23	0.04	0.04	0.12	0.21
CHAN	TRANSVERSE	0.01	0.01	0.01	0.01	0.43	0.53	0.09	0.06	0.09	0.16	0.26	0.54
	VERTICAL	0.07	0.01	0.02	0.02	0.03	0.10	0.04	0.07	0.02	0.09	0.13	0.10
	RADIAL	0.56	0.45	0.95	1.16	0.70	4.68	2.39	1.67	0.75	0.28	2.33	4.92
CHIN	TRANSVERSE	0.27	0.26	0.60	2.00	7.04	1.90	3.24	1.07	3.28	1.27	5.92	5.73
	VERTICAL	1.85	1.06	0.67	2.38	1.24	0.96	0.43	2.00	0.87	0.52	3.99	0.71
	RADIAL	0.64	0.24	1.44	0.84	0.96	0.41	2.05	6.82	0.78	1.39	1.19	0.85
GIYA	TRANSVERSE	0.60	0.42	0.49	0.65	2.54	3.09	2.38	0.31	2.39	3.64	1.16	0.18
	VERTICAL	0.01	0.01	1.83	1.39	0.84	1.44	0.62	1.98	0.13	0.43	2.53	0.50
	RADIAL	0.39	1.32	1.02	0.43	0.01	4.26	2.44	1.44	0.23	0.47	4.37	3.60
KHUR	TRANSVERSE	0.87	0.13	0.67	1.14	1.98	6.27	2.81	2.51	1.17	1.03	0.95	2.15
	VERTICAL	0.79	0.45	0.16	1.21	0.40	0.17	1.39	3.63	0.62	0.69	2.28	0.86
	RADIAL	1.00	1.00	1.00	1.00	1.00	1.00	1.00	1.00	1.00	1.00	1.00	1.00
PRAT	TRANSVERSE	1.00	1.00	1.00	1.00	1.00	1.00	1.00	1.00	1.00	1.00	1.00	1.00
	VERTICAL	1.00	1.00	1.00	1.00	1.00	1.00	1.00	1.00	1.00	1.00	1.00	1.00
	RADIAL	0.37	0.10	0.49	0.20	0.77	1.01	1.49	1.41	2.82	2.11	6.67	3.99
RAJG	TRANSVERSE	0.22	0.22	0.16	0.69	0.45	3.65	3.52	3.06	2.05	1.83	3.55	3.65
	VERTICAL	3.58	0.70	0.61	0.70	0.50	0.46	1.01	2.55	0.26	0.81	6.10	2.10

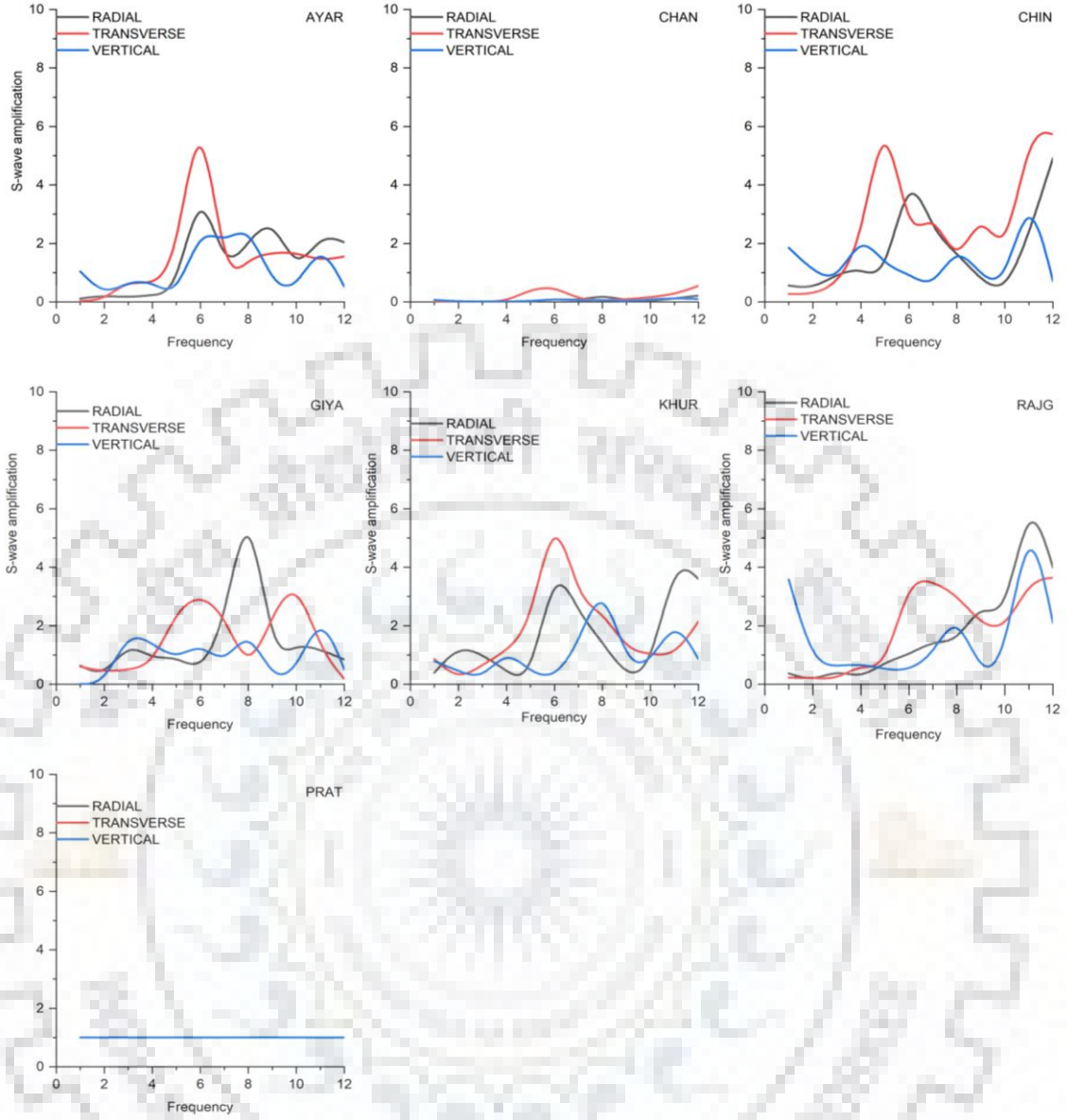

Figure 4.8: S-wave spectral ratio amplification for earthquake occurred south-east of PRAT on 28-07-2012 relative to PRAT station.

Table 4.9: S-wave spectral ratio amplification for earthquake occurred north-west of PRAT on 11-02-2013 relative to PRAT station.

FREQUENCY		1	2	3	4	5	5	6	7	8	10	11	12
	RADIAL	0.74	0.43	3.13	0.14	0.34	0.94	1.06	1.40	3.40	0.46	0.47	2.70
AYAR	TRANSVERSE	0.17	0.64	4.53	0.95	0.08	0.46	1.55	0.81	1.23	1.03	1.63	2.21
	VERTICAL	1.20	1.51	0.99	4.26	0.65	0.58	0.92	0.44	1.28	1.04	0.83	1.18
	RADIAL	0.59	0.09	0.03	0.30	2.02	0.66	1.66	7.65	2.36	0.55	2.83	2.05
CHAN	TRANSVERSE	0.33	0.11	3.57	0.23	0.14	1.89	1.08	5.01	1.62	2.27	0.72	2.83
	VERTICAL	0.12	0.14	0.05	0.33	0.58	0.09	0.60	0.20	0.30	0.47	1.13	0.57
	RADIAL	0.23	0.01	0.58	0.59	0.20	0.59	1.59	1.61	0.63	0.63	0.31	2.31
CHIN	TRANSVERSE	0.11	0.10	3.99	0.37	0.25	0.40	0.33	2.93	0.56	0.43	0.23	0.22
	VERTICAL	0.48	0.31	0.13	2.86	0.24	0.77	0.44	0.76	0.38	0.36	0.44	0.16
	RADIAL	2.09	0.68	3.57	3.79	3.28	8.01	7.36	8.01	3.35	3.75	1.34	1.24
GIYA	TRANSVERSE	2.49	2.94	2.12	5.56	3.08	7.27	8.72	3.13	5.82	3.48	3.04	3.51
	VERTICAL	1.42	0.80	2.72	5.16	4.68	2.90	7.11	4.31	6.17	3.36	3.54	5.21
	RADIAL	0.74	0.43	3.13	0.14	0.34	0.94	1.06	1.40	3.40	0.46	0.47	2.70
KHUR	TRANSVERSE	0.17	0.64	4.53	0.95	0.08	0.46	1.55	0.81	1.23	1.03	1.63	2.21
	VERTICAL	1.20	1.51	0.99	4.26	0.65	0.58	0.92	0.44	1.28	1.04	0.83	1.18
	RADIAL	0.10	0.86	2.93	0.27	0.48	0.51	0.89	0.66	3.03	0.49	0.74	1.06
NEWT	TRANSVERSE	0.21	0.87	5.91	0.51	0.00	1.33	0.39	3.39	0.47	0.30	0.47	0.44
	VERTICAL	1.75	1.60	1.04	1.65	0.99	0.62	0.28	0.42	2.02	0.65	0.50	0.07
	RADIAL	1.00	1.00	1.00	1.00	1.00	1.00	1.00	1.00	1.00	1.00	1.00	1.00
PRAT	TRANSVERSE	1.00	1.00	1.00	1.00	1.00	1.00	1.00	1.00	1.00	1.00	1.00	1.00
	VERTICAL	1.00	1.00	1.00	1.00	1.00	1.00	1.00	1.00	1.00	1.00	1.00	1.00
	RADIAL	1.78	1.94	1.46	1.56	2.96	3.36	2.03	1.01	5.83	2.24	3.29	2.52
RAJG	TRANSVERSE	2.63	4.95	4.72	4.72	0.80	1.07	4.91	6.88	0.48	2.91	2.78	2.79
	VERTICAL	2.07	4.59	3.62	4.34	3.56	2.78	5.22	3.19	2.38	3.63	3.24	0.68
	RADIAL	0.06	0.02	0.13	0.15	0.15	0.10	0.29	0.43	0.65	0.40	1.21	2.86
SIRA	TRANSVERSE	0.18	0.23	1.64	0.09	0.19	0.82	0.14	0.94	0.08	0.31	0.25	0.42
	VERTICAL	0.52	0.39	0.09	0.83	0.35	0.11	0.13	0.12	1.56	0.11	0.81	0.56
	RADIAL	1.91	0.68	1.61	0.87	0.85	0.80	1.69	3.15	2.68	1.81	3.50	3.94
SIRK	TRANSVERSE	2.34	2.42	2.23	0.79	0.54	1.13	0.33	4.92	0.95	1.51	0.94	1.75
	VERTICAL	1.26	0.77	2.73	1.94	1.75	0.82	1.32	2.06	2.30	1.62	2.85	0.94
	RADIAL	0.00	0.00	0.00	0.00	0.00	0.00	0.00	0.00	0.00	0.00	0.00	0.00
SURK	TRANSVERSE	0.00	0.00	0.00	0.00	0.00	0.00	0.00	0.00	0.00	0.00	0.00	0.00
	VERTICAL	0.00	0.00	0.00	0.00	0.00	0.00	0.00	0.00	0.00	0.00	0.00	0.00
	RADIAL	0.64	0.46	0.72	0.28	0.57	0.88	2.40	2.77	0.82	2.34	2.26	2.79
VINA	TRANSVERSE	0.83	1.26	0.45	0.48	0.16	0.43	1.72	1.81	1.59	0.75	1.45	0.34
	VERTICAL	0.50	0.68	0.80	2.39	2.08	1.67	2.35	0.64	0.51	1.17	0.74	1.37

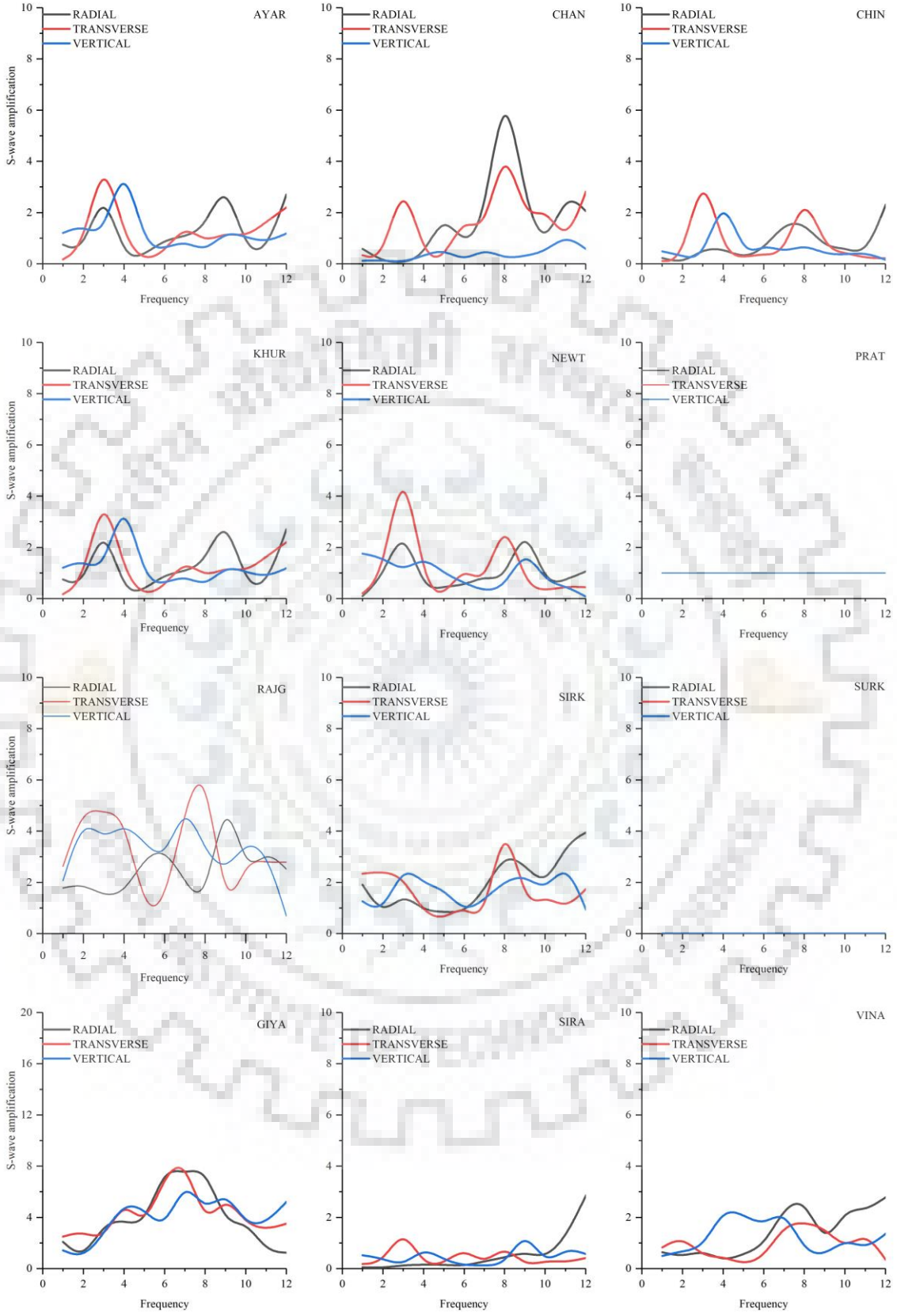

Figure 4.9: S-wave spectral ratio amplification for earthquake occurred north-west of PRAT on 11-02-2013 relative to PRAT station.

Table 4.10: S-wave spectral ratio amplification for earthquake occurred north-east of PRAT on 18-07-2015 relative to PRAT station.

FREQUENCY		1	2	3	4	5	5	6	7	8	10	11	12
	RADIAL	0.36	0.36	2.13	3.37	4.17	1.79	7.28	3.60	1.29	1.18	1.46	3.15
AYAR	TRANSVERSE	1.07	0.33	0.68	0.74	3.71	2.50	1.94	2.32	0.06	1.51	0.29	5.94
	VERTICAL	1.07	0.10	0.40	0.68	1.79	1.82	3.60	1.76	0.08	0.78	0.72	2.12
	RADIAL	0.00	0.00	0.03	0.02	0.43	0.01	0.20	0.03	0.10	0.04	0.01	0.04
CHAN	TRANSVERSE	0.03	0.00	0.17	0.02	0.09	0.02	0.20	0.38	0.04	0.16	0.02	0.13
	VERTICAL	1.23	1.46	0.82	0.76	1.40	0.59	4.51	0.51	0.38	1.65	1.73	1.20
	RADIAL	0.51	0.26	3.72	3.66	4.75	1.31	3.79	0.32	3.42	0.51	0.80	3.08
KHUR	TRANSVERSE	0.60	0.33	3.92	2.96	3.95	0.63	3.05	1.16	1.06	1.26	1.16	2.72
	VERTICAL	0.70	1.01	0.32	0.08	1.25	0.87	2.65	1.26	0.36	0.68	0.30	3.36
	RADIAL	0.29	0.37	2.18	1.34	1.57	0.63	1.68	0.89	4.41	0.88	0.80	1.66
NEWT	TRANSVERSE	1.32	0.06	2.98	0.87	2.92	0.63	1.11	1.18	1.19	0.95	1.57	1.42
	VERTICAL	1.22	1.07	0.75	1.15	0.57	0.77	1.01	0.54	0.26	0.90	0.28	0.78
	RADIAL	1.00	1.00	1.00	1.00	1.00	1.00	1.00	1.00	1.00	1.00	1.00	1.00
PRAT	TRANSVERSE	1.00	1.00	1.00	1.00	1.00	1.00	1.00	1.00	1.00	1.00	1.00	1.00
	VERTICAL	1.00	1.00	1.00	1.00	1.00	1.00	1.00	1.00	1.00	1.00	1.00	1.00
	RADIAL	0.21	0.11	1.39	1.59	1.70	0.59	2.17	1.10	0.36	0.43	0.28	0.26
RAJG	TRANSVERSE	0.31	0.23	1.65	0.22	1.74	0.57	1.52	3.51	0.60	0.96	0.06	1.77
	VERTICAL	0.79	1.03	0.73	0.43	0.64	0.10	1.00	0.26	0.18	0.09	0.19	0.91
	RADIAL	0.10	0.33	1.06	2.64	7.62	0.50	2.24	1.06	3.01	0.67	0.74	0.97
SIRA	TRANSVERSE	0.30	0.13	1.26	0.99	0.79	0.22	0.27	4.43	0.05	1.14	1.43	2.58
	VERTICAL	1.63	2.10	0.34	0.48	0.97	0.17	2.13	1.10	0.21	0.73	0.99	0.51
	RADIAL	0.13	0.07	0.61	0.41	4.51	0.35	1.98	0.65	2.19	0.67	0.35	0.44
SIRK	TRANSVERSE	0.29	0.18	4.11	0.34	1.06	0.29	0.30	0.41	0.54	1.49	0.69	3.09
	VERTICAL	0.55	0.27	0.27	0.30	0.28	0.19	0.63	0.17	0.12	0.18	0.08	0.50
	RADIAL	0.28	0.02	3.19	1.95	1.63	0.48	2.52	2.04	4.41	1.76	1.36	2.00
VINA	TRANSVERSE	0.46	0.05	1.51	0.69	1.99	1.49	1.13	1.76	1.22	4.06	1.39	1.16
	VERTICAL	0.29	1.37	0.72	1.47	1.20	0.69	2.57	1.30	0.28	0.72	1.16	1.37
	RADIAL	1.91	0.68	1.61	0.87	0.85	0.80	1.69	3.15	2.68	1.81	3.50	3.94
SIRK	TRANSVERSE	2.34	2.42	2.23	0.79	0.54	1.13	0.33	4.92	0.95	1.51	0.94	1.75
	VERTICAL	1.26	0.77	2.73	1.94	1.75	0.82	1.32	2.06	2.30	1.62	2.85	0.94
	RADIAL	0.00	0.00	0.00	0.00	0.00	0.00	0.00	0.00	0.00	0.00	0.00	0.00
SURK	TRANSVERSE	0.00	0.00	0.00	0.00	0.00	0.00	0.00	0.00	0.00	0.00	0.00	0.00
	VERTICAL	0.00	0.00	0.00	0.00	0.00	0.00	0.00	0.00	0.00	0.00	0.00	0.00
	RADIAL	0.64	0.46	0.72	0.28	0.57	0.88	2.40	2.77	0.82	2.34	2.26	2.79
VINA	TRANSVERSE	0.83	1.26	0.45	0.48	0.16	0.43	1.72	1.81	1.59	0.75	1.45	0.34
	VERTICAL	0.50	0.68	0.80	2.39	2.08	1.67	2.35	0.64	0.51	1.17	0.74	1.37

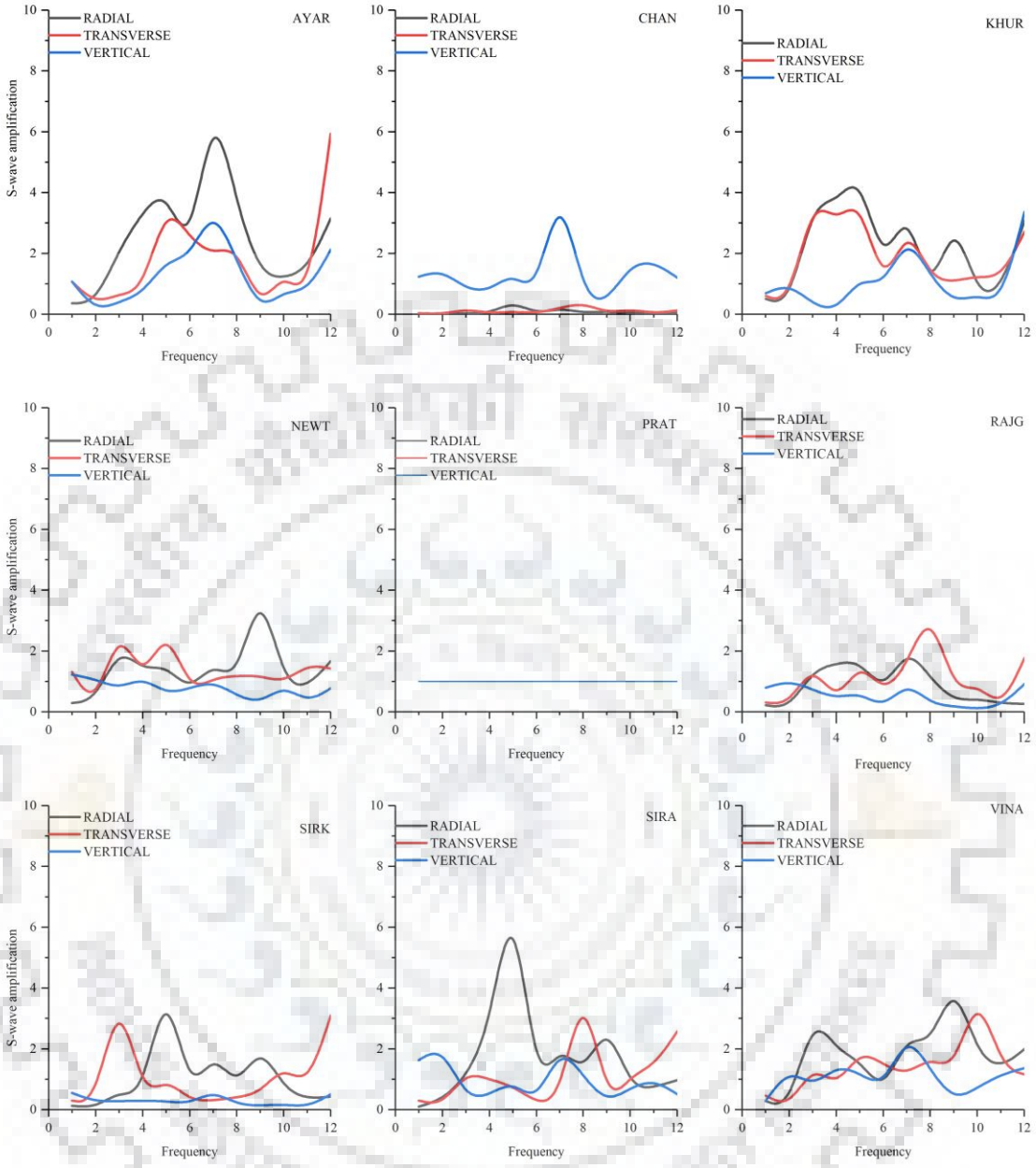

Figure 4.10: S-wave spectral ratio amplification for earthquake occurred north-east of PRAT on 18-07-2015 relative to PRAT station.

Table 4.11 S-wave spectral ratio amplification for earthquake occurred south-east of PRAT on 01-12-2016 relative to PRAT station.

FREQUENCY		1	2	3	4	5	5	6	7	8	10	11	12
	RADIAL	1.42	0.94	1.12	0.78	0.87	2.28	3.16	3.20	4.64	1.46	1.20	2.77
AYAR	TRANSVERSE	0.20	0.91	2.87	4.08	2.04	3.39	2.03	5.45	4.25	4.07	3.44	1.31
	VERTICAL	0.72	4.87	5.80	0.52	0.86	2.41	4.58	0.88	1.23	3.77	3.74	1.90
	RADIAL	0.15	0.60	2.30	0.49	1.05	6.47	3.93	5.33	5.79	9.76	4.95	3.97
CHAN	TRANSVERSE	0.21	1.28	1.39	2.73	2.55	4.91	6.37	8.55	8.67	8.95	5.56	3.52
	VERTICAL	1.79	5.58	5.59	0.32	2.05	2.11	6.66	1.44	1.56	1.60	5.29	2.03
	RADIAL	0.50	0.43	4.63	0.46	0.11	0.23	0.26	3.36	2.07	0.75	1.86	1.66
CHIN	TRANSVERSE	0.14	1.07	1.37	0.74	0.74	4.25	3.49	1.54	1.13	1.13	1.74	1.17
	VERTICAL	0.65	2.44	2.56	2.07	0.68	1.57	2.55	0.55	0.39	1.36	1.52	0.71
	RADIAL	0.87	0.68	4.38	0.83	0.65	0.90	2.07	3.47	4.43	0.76	1.94	0.78
GIYA	TRANSVERSE	0.37	1.00	0.84	2.64	0.52	0.35	3.83	1.36	4.27	0.90	2.41	0.40
	VERTICAL	2.18	1.17	3.00	4.41	1.08	1.04	1.12	0.50	0.09	1.20	2.27	0.24
	RADIAL	0.05	0.06	0.02	0.01	0.03	0.02	0.06	0.17	0.06	0.03	0.04	0.00
NEWT	TRANSVERSE	0.17	0.26	0.03	0.21	0.12	0.11	0.58	0.47	0.71	0.25	0.03	0.04
	VERTICAL	1.20	1.64	0.00	0.89	1.11	0.38	1.99	0.99	0.41	0.35	1.13	0.13
	RADIAL	1.00	1.00	1.00	1.00	1.00	1.00	1.00	1.00	1.00	1.00	1.00	1.00
PRAT	TRANSVERSE	1.00	1.00	1.00	1.00	1.00	1.00	1.00	1.00	1.00	1.00	1.00	1.00
	VERTICAL	1.00	1.00	1.00	1.00	1.00	1.00	1.00	1.00	1.00	1.00	1.00	1.00
	RADIAL	1.13	0.70	1.05	0.09	0.33	0.53	0.85	1.56	0.59	0.55	1.28	0.19
RAJG	TRANSVERSE	0.48	0.70	1.36	2.72	1.01	0.47	1.20	1.72	3.29	1.20	0.65	3.20
	VERTICAL	2.14	3.06	5.08	0.37	1.21	0.33	1.12	0.48	0.53	0.74	0.54	0.26
	RADIAL	0.33	0.28	1.23	0.27	0.42	0.75	0.77	1.92	6.92	0.97	6.11	1.49
SIRA	TRANSVERSE	0.06	0.43	1.89	2.35	0.73	0.52	3.62	2.35	4.95	3.29	1.99	6.68
	VERTICAL	1.52	1.90	8.18	1.56	0.32	0.32	1.90	1.45	0.99	7.35	1.76	1.03
	RADIAL	0.25	0.10	0.76	0.03	0.10	0.36	0.68	0.68	0.83	0.43	0.36	0.82
SIRK	TRANSVERSE	0.19	0.66	0.44	0.56	0.60	0.32	2.76	1.68	1.90	1.37	1.28	3.77
	VERTICAL	0.92	0.32	1.03	0.35	0.27	0.14	1.19	0.15	0.13	0.68	0.22	0.41
	RADIAL	1.65	1.01	4.24	0.68	0.72	1.18	1.36	3.16	1.26	0.68	2.67	1.13
SURK	TRANSVERSE	0.37	1.36	1.51	1.02	1.17	1.10	1.29	2.17	4.50	3.02	4.94	3.22
	VERTICAL	1.96	4.23	4.23	0.88	1.37	0.81	0.73	0.35	0.23	0.89	1.75	0.63

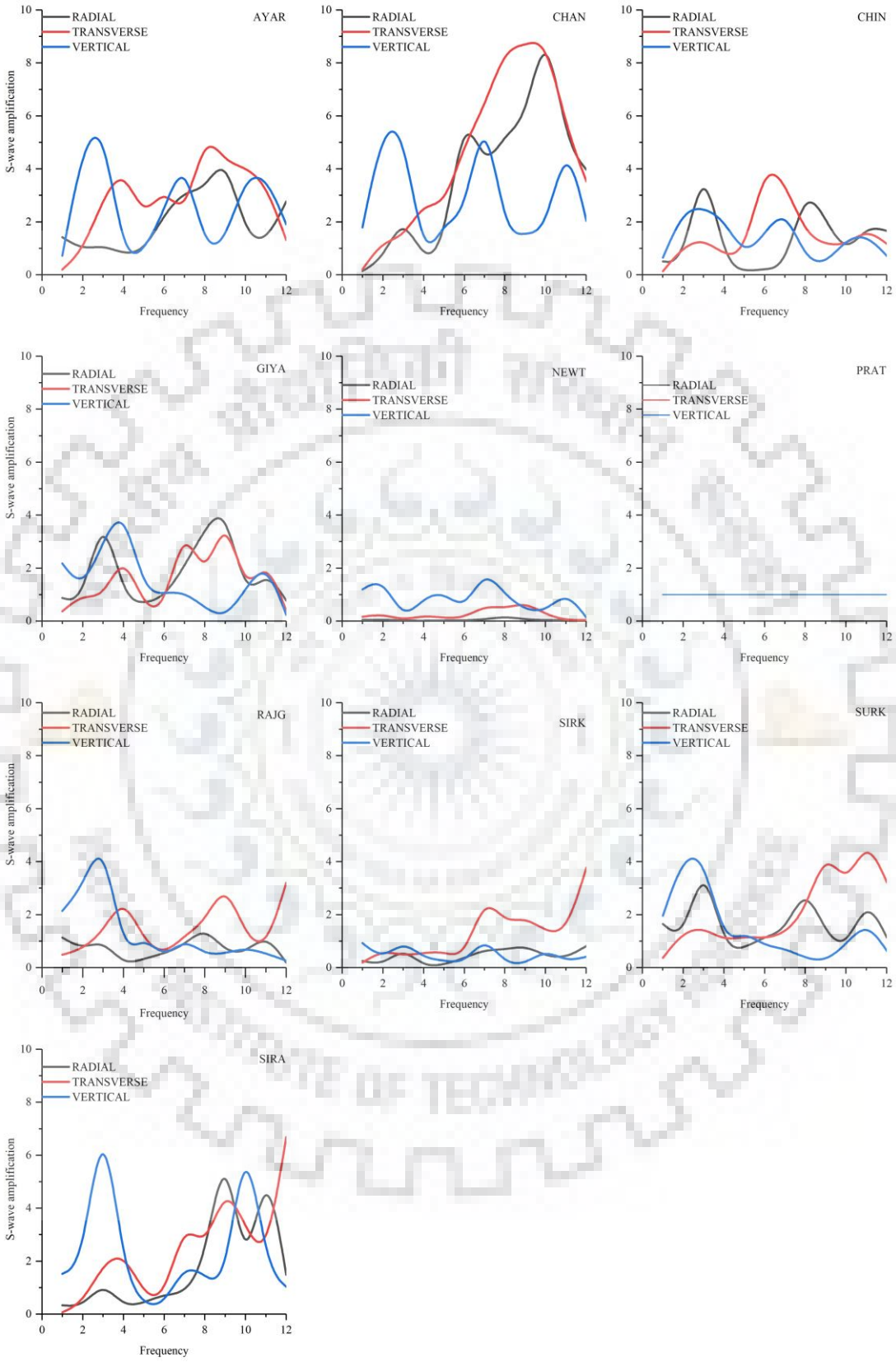

Figure 4.11: S-wave spectral ratio amplification for earthquake occurred south-east of PRAT on 01-12-2016 relative to PRAT station.

Chapter-5 Conclusions

Based on the analysis of six and four local earthquakes used for the site amplification in the Garhwal Himalayas using H/V spectral ratio and S-wave spectral ratio method following broad conclusions has been drawn from the study:

Using HVSR method, maximum amplification is obtained in the frequency between 2 Hz to 5 Hz and the amplification values decreases beyond 5 Hz. The amplification factors obtained are non-linear functions of the frequency. By HVSR method, fundamental frequencies and the corresponding amplification factor for the site has been obtained. It has been observed that HVSR method underestimates the amplification factor at higher frequencies, more than 5 Hz.

Using S-wave spectral ratio method, site amplification obtained in the radial and transverse components shows similar frequency dependent trend at majority of sites with PRAT site being a reference site. The different components of the site amplification were compared and it was found that the vertical component shows low amplification as compared to the radial and transverse components above frequency of 5 Hz. Nearly same order of amplification is observed at the sites in the same frequency range as obtained in HVSR method. Table 5.1 shows maximum amplification occurring at stations corresponding to frequency range obtained by the two methods due to various earthquakes.

The results obtained can be used for seismic hazard analysis and the wave velocity can be obtained using the fundamental frequencies. More earthquake data can be further used for the S-wave Spectral Ratio method.

Table 5.1: Amplification factors obtained by HVSR and S-wave Spectral Ratio methods.

Station	HVSR order of amplification	HVSR frequency range	S-wave method order of amplification	S-wave method frequency range
AYAR	6	3-5	6	4-7
CHAN	10	7-9	9	7-9
CHIN	5	4-6	6	3-6
GIYA	7	2-4	4	3-5
KHUR	8	3-5	6	4-6
NEWT	4	3-5	4	2-4
PRAT	6	2-4	-	-
RAJG	5	2-3	4	2-4
SIRA	2	4-6	6	3-5
SIRK	5	2-5	3	2-4
SURK	3	0-2	3	3-5
VINA	3	1-3	3	1-3

References

1. Aki, K., and Phillip, W. S. (1986). "Site amplification of coda waves from local earthquakes in central California." *Bulletin of the Seismological Society of America*, 76(3), 627-648.

2. Arai, H., and Tokimatsu, K. (2005). "S-wave Velocity profiling by joint inversion of microtremor dispersion curve and horizontal to vertical spectrum." *Bulletin of the Seismological Society of America*, 95(5), 1766–1778.

3. Bonilla, L. F., Steidl, J. H., Lindley, G. T., Tumarkin, G., and Archuleta, R. J. (1997). "Site amplification in the San Fernando Valley, California: variability of site effect estimation using the S-wave, coda wave and H/V method." *Bulletin of the Seismological Society of America*, 87(3), 710-730.

4. Boore, D. M. (2003). "Simulation of Ground motion using the Stochastic Method." *Pure appl. Geophys*, 160(3), 635–676.

5. Boore, D. M., and William, B. J. (1997). "Site amplification for generic rock sites." *Bulletin of the Seismological Society of America*, 87(2), 327-341.

6. Borcherdt, R. D. (1970). "Effects of local geology on ground motion near San Francisco Bay." *Bulletin of the Seismological Society of America*, 60(1), 29-61.

7. Castro, R. R., Mucciarelli, M., Pacor, F., and Petrrungaro, C. (1997). "S-wave site response estimates using horizontal to vertical spectral ratios." *Bulletin of the Seismological Society of America*, 87(1), 256-260.

8. Chopra, S., Kumar, D., Rastogi, B. K., Choudhary, P., Yadav, R. B. S. (2013). "Estimation of site amplification functions in Gujarat region." *Nat Hazards*, 65, 1135–1155.

9. Chopra, S., Kumar, V., Suthar, A., and Kumar, P. (2012). "Modelling of strong ground motions for 1991 Uttarkashi, 1999 Chamoli earthquakes and a hypothetical great earthquake in Garhwal –Kumaun Himalaya." *Nat Hazards*, 64, 1141–1159.

10. Kato, K., Aki, K., and Takemura, M. (1995). "Site amplification from coda waves: Validation and application to S-wave site response." *Bulletin of the Seismological Society of America*, 85(2), 467-477.

11. Nakamura, Y. (1989). "A method for dynamic characteristics estimation of subsurface using microtremor on the ground surface." *Q.R. of R.T.R.I.*, 30(1), 25–33.

12. Seekins, C. L., Wennerberg, L., Margheriti, L., and Liu, H. P. (1996). "Site amplification at five locations in San Francisco: A comparison of S-wave, coda and microtremors." *Bulletin of the Seismological Society of America*, 86(3), 627-635.

13. *Seisan Explorer Developer version 2.5.5* [Computer Software] University of Bergen, Department of Earth Science, Bergern, Norway.

14. Sharma, A. (2015). "Estimation of Site amplification in Arunachal Himalaya using coda waves." Department of Earthquake Engineering, M. Tech. Dissertation. IIT Roorkee.

15. Sudhakar, A. (2012). "Site amplification characteristics of Garhwal and Lesser Himalaya using S-wave and HVSR method." Department of Earthquake Engineering, M. Tech. Dissertation. IIT Roorkee.